Effects of two centuries of global environmental variation on phenology and physiology of *Arabidopsis thaliana*

Victoria L. DeLeo[1,2], Duncan N. L. Menge[4], Ephraim M. Hanks[5], Thomas E. Juenger[6], Jesse R. Lasky[3,4,7]

[1]Huck Institutes of the Life Sciences | Plant Biology
Pennsylvania State University
University Park, PA 16802

[2]Corresponding author
Email: vldeleo@psu.edu

[3]Department of Biology
Pennsylvania State University
University Park, PA 16802

[4]Department of Ecology, Evolution, and Environmental Biology
Columbia University
New York, NY 10027

[5]Department of Statistics
Pennsylvania State University
University Park, PA 16802

[6]Department of Integrative Biology
University of Texas at Austin
Austin, TX 78712

[7]Earth Institute
Columbia University
New York, NY 10025

Abstract

Intraspecific diversity arises from genetic and plastic responses to the environment. Immense natural history collections allow comprehensive surveys of intraspecific diversity across a species range through centuries of environmental variation. Using 216 years of *Arabidopsis thaliana* samples, we tested if traits exhibit coordinated variation and hypothesized adaptive responses to climate gradients. We used spatially varying coefficient models to quantify region-specific trends. Traits generally showed little coordination. However, C:N was low for summer versus spring-collected plants, consistent with a life history-physiology axis from slow-growing winter annuals to fast-growing spring/summer annuals. Collection date was later in more recent years in many regions, possibly because these populations shifted toward more spring (as opposed to fall) germination. δ^{15}N decreased over time across most of the range, consistent with predictions based on anthropogenic changes. Regional heterogeneity in phenotype trends indicates complex responses to spatial and temporal climate shifts potentially arising from variation in local adaptation and plasticity.

Introduction

Fitness critically depends on an organism's response to environmental variability. Anthropogenic global environmental change is resulting in dramatic changes in phenotypes of many organisms. Despite general patterns of species' poleward range shifts and advancement of temperate spring phenology (Parmesan & Yohe), populations and individuals often differ in their responses to changing climates (Both *et al.* 2004; CaraDonna *et al.* 2014). These diverse responses could be caused by geographic variation in the rate of environmental change or by intraspecific genetic variation, clouding our understanding of climate impacts. Quantifying the spatial patterns of responses to environmental gradients can put temporal trends in context as well as reveal adaptive phenotypic variation across the species range.

Organisms respond to environmental stressors in diverse ways, including life history, phenology, and physiology. In seasonal locations, phenology dictates the environment encountered during vulnerable stages. Plant phenology and development are primarily limited by moisture, temperature, and photoperiod (Wilczek *et al.* 2009; Burghardt *et al.* 2015). Warmth usually increases growth rate, however cold temperatures in critical periods can advance flowering time through a process known as vernalization. Rapid development and reproduction can allow plants to escape drought, a strategy employed by some genotypes of our study species *Arabidopsis thaliana* (hereafter, Arabidopsis, Kenney *et al.* 2014). Other genotypes exhibit drought avoidance by minimizing water loss (e.g. through stomatal closure) and maximizing water uptake (Ludlow 1989; Kenney *et al.* 2014). Fast life histories can allow spring or summer annual life cycles, where a plant germinates and flowers within a single season, while slow life histories and vernalization requirements result in a winter annual cycle, where a plant germinates in the fall and flowers the following spring.

Standardized metrics are needed to compare ecologically relevant phenological variation among sites of different climate timing and at different latitudes. Photothermal units (PTU) integrate developmental time under favorable temperatures and light across a growing season and account for much of the environmental influence on flowering dates (Wilczek *et al.* 2009; Brachi *et al.* 2010). Thus, PTUs may help capture genetic differences in phenology across environments. Measures of developmental time standardized to environmental conditions can better capture genetic variation in development compared to raw flowering dates in Arabidopsis (Brachi *et al.* 2010).

Beyond flowering time, plant physiological response to environment is partly reflected in leaf isotope and nutrient composition, traits with high intraspecific genetic and plastic variation (Nienhuis *et al.* 1994; Chardon *et al.* 2010). $\Delta^{13}C$, which measures discrimination against ^{13}C in photosynthesis, is an indicator of pCO2 within leaves (C_i) relative to atmospheric pCO2 (C_a) (Farquhar *et al.* 1982). C_i declines when stomata are closed, which may occur under drought, while C_a declines with elevation. Thus, we expect $\Delta^{13}C$ to increase in moist environments and decrease with elevation (Farquhar *et al.* 1982; Diefendorf *et al.* 2010; Zhu *et al.* 2010).

Leaf nitrogen physiology is another important aspect of environmental response, since leaf nitrogen is important to photosynthetic capacity (Stocking & Ongun 1962; Evans 1989) and photorespiration (Rachmilevitch *et al.* 2004). At the community level, leaf N (proportion of mass) generally increases with mean annual temperature (Reich & Oleksyn 2004; Ordoñez *et al.* 2009), and increases with greater precipitation (Reich *et al.* 2003). Lower nitrogen concentration leaves (high C:N, low proportion N) are found in drier and in hotter areas, in part because of investment in non-photosynthetic leaf features, especially veins (Blonder *et al.* 2011; Sack *et al.* 2012). Leaf $\delta^{15}N$, or the fraction of ^{15}N over total nitrogen in a leaf, can be affected by the same resource acquisition strategies and is related to leaf N

(Stock & Evans 2006). However, leaf N and $\delta^{15}N$ may also reflect deposition and biogeochemical cycling (e.g. Pardo *et al.* 2007), complicating biological explanations. In this study, we used the ratio of carbon to nitrogen in the leaf (C:N) to capture leaf nitrogen investments.

The physiological, morphological, or phenological traits plants use to cope with varied environments often are subject to tradeoffs. When resources are abundant (high nutrient, ample water, warmth), functional traits enabling rapid growth and low investment in tissues may be favored, leading to low leaf C:N ratio. When resources are limited, slow growth and costlier, longer-lived tissues may be favored (Reich 2014). Accordingly, the winter annual phenology of northern Arabidopsis ecotypes described above could be explained by a slow growth strategy, while a fast growth strategy could lead to drought escape in arid regions. In addition, this fast growth could lead to higher leaf $\Delta^{13}C$ through increased photosynthetic and transpiration rates. The leaf economic spectrum (LES) predicts that multiple dimensions of trait variation are coordinated to reflect a single life history and physiology axis from fast to slow that also corresponds to changes in dominant vegetation types across environments (Wright *et al.* 2004; Reich 2014), though the association of LES traits with climate may be weaker within species (Wright & Sutton-Grier 2012). We hypothesized that phenotype-environment correlations would follow LES or fast-slow predictions (Table 1).

Table 1: Hypothesized responses of phenotypes to temperature, rainfall, or year. Year trends are predicted due to elevated CO_2, nitrogen deposition, or elevated temperatures.

	Temperature	Rainfall	Year
$\Delta^{13}C$	+	+ [7]	+ [9]
$\delta^{15}N$	+ [1,5]	- [1,5]	- [8, 4]
C:N	- [6]	- [2]	+ [3,8]
Photothermal Units	+ or no change	+	No change
Collection Date	-	+	-

(Amundson *et al.* 2003[1]; Wright *et al.* 2004[2]; Reich *et al.* 2006[3]; Pardo *et al.* 2007[4]; Craine *et al.* 2009[5]; Ordoñez *et al.* 2009[6]; Diefendorf *et al.* 2010[7]; McLauchlan *et al.* 2010[8]; Drake *et al.* 2017[9])

Museum collections offer broadly distributed sampling in space and time to test the relationships between these phenotypes and climate (Willis *et al.* 2017; Lang *et al.* 2018). Variation in herbarium collection dates can be a reliable proxy for variation in phenology (Miller-Rushing *et al.* 2006; MacGillivray *et al.* 2010; Davis *et al.* 2015). Here, we leverage the immense fieldwork underlying natural history collections to understand how intraspecific diversity is structured through time and along spatiotemporal climate gradients. We combine these records with global gridded climate data to ask three questions:

1. Does intraspecific trait variation among wild individuals fall along a single coordinated life history-physiology axis? Alternatively, is trait variation higher dimensional?
2. Do Arabidopsis life history and physiology vary across spatial environmental gradients, suggesting adaptive responses to long-term environmental conditions?
3. Have Arabidopsis life history and physiology changed over the last two centuries? In particular, have changes tracked climate fluctuations, suggesting adaptive responses?

Material and methods

Our samples included 3300 *Arabidopsis thaliana* herbarium and germplasm accessions with known collection date between 1794 and 2010 from the native range of Arabidopsis in Europe, the Middle East, Central Asia, and North Africa (Hoffmann 2002). For each herbarium specimen (n = 3163 of the total 3300) we visually verified species identification, flowering and fruiting reproductive status. Samples that were only fruited/senesced (n = 40) and samples that were only flowering (n = 96) as well as samples that had neither open flowers nor fruits (n = 10) were excluded to select for a more uniform development stage. Since progression of plant development involves reallocation of nutrients, C:N should be assessed at a consistent developmental stage. We also excluded dozens of misidentified specimens. Our effort highlights the risks of using unverified natural history collection data in online databases. Wild-collected germplasm accessions with known collection date and location were included from the Arabidopsis Biological Resource Center (https://abrc.osu.edu/).

We removed and pulverized leaf samples of 470 herbarium specimens and sent them to the UC-Davis Stable Isotope Facility. In total, we obtained δ^{15}N values for 456 accessions, δ^{13}C values for 454 accessions, C:N ratios for 455 accessions, and proportion N values for 455 accessions. Because atmospheric δ^{13}C has changed dramatically over the time period of this study, we converted leaf δ^{13}C to Δ^{13}C using a common estimate of the atmospheric δ^{13}C time series (McCarroll & Loader 2004) from 1850 to 2000, continuing linear extrapolation beyond 2000, using the 1850 value for earlier specimens, and the equation of Farquhar et al. (1989)

$$\Delta = \frac{\delta_a - \delta_p}{1+\delta_p}.$$

where δ_a is the isotope ratio in the atmosphere and δ_p is the isotope ratio in plant tissue (ratios relative to a standard).

We selected climate variables based on knowledge of critical Arabidopsis developmental times and likely environmental stressors: average temperature in April (AprilMean in the models), minimum temperature in January (JanMinimum), July aridity index (AI) (Hoffmann 2002; Lasky *et al.* 2012; Fournier-Level *et al.* 2013; Wilczek *et al.* 2014). Aridity index was calculated from July precipitation divided by July PET (United Nations Environment Program 1997). These climate gradients were generally not strongly correlated (July Aridity to April Mean Temperature r^2 = .09; July Aridity to January Minimum Temperature r^2 = .003; January Minimum Temperature to April Mean Temperature r^2 = .44 by linear regression). Temperature, precipitation, and PET values came from the Climate Research Unit time series dataset (New *et al.* 2000).

To estimate accumulated photothermal units (PTU) at date of collection, we used the equation of Burghardt et al. (2015) to model the hourly temperature values for the accumulation of sunlight degree hours between January 1 and dusk on the day of collection at each accession's coordinate. Daylength was approximated with the R package geosphere (Hijmans 2017). Monthly temperature values for the period 1900-2016 came from the Climate Research Unit time series dataset (New *et al.* 2000). PTUs were only calculated for specimens collected after 1900. Daily temperatures were interpolated from monthly temperatures using the function splinefun in R on the "periodic" setting.

Arabidopsis displays substantial genetic diversity in environmental response between genotypes from different regions (e.g. Lasky *et al.* 2018). Thus, we employed a regression model with spatially varying coefficients (generalized additive models, GAMs) to account for regional differences in responses to environment, much of which may have a genetic component (Wood 2006; Wheeler & Waller 2009). GAMs allow fitting of parameters that vary smoothly in space (i.e. parameter surfaces) and can thus

capture spatially varying relationships between predictors and the response of interest. To assess how phenotypes have changed across the last few centuries, we first tested a model with a spatially varying intercept (SVI) and a spatially-varying coefficient model for the effect of year, allowing for geographic variation in temporal trends. We refer to these subsequently as "year models". These models included all specimens with phenotype data.

Next, to assess how temporal fluctuations in climate drive phenotypic change, we fit models with an SVI and standardizing climate conditions from all years (1901-2016) within a grid cell to unit standard deviations and mean zero ("temporal models"). These models only included specimens from after 1900, when we had data on monthly climate from CRU.

$$Phenotype_{ij} = \beta_1 year\_{}_{dev,\,ij} + \beta_2 AI\_{}_{dev,\,ij} + \beta_3 JanMinimum\_{}_{dev,\,ij} + \beta_4 AprilMean\_{}_{dev,\,ij} + \mu_j + error_{ij}$$

In this model, the subscript j denotes location and i denotes year of collection. The SVI is denoted by μ_i , where the "j" subscript indicates that the intercept varies with location. The errors are assumed to be independent, be normally distributed, and have constant variance.

Third, to study spatial variation in phenotypes in response to spatial climate gradients, we fit models with spatially varying effects of climate, and with scaled long-term, 50-year climate averages at each location and scaled year of collection as covariates ("spatial models") (Hijmans *et al.* 2005). In these models, the intercept was not allowed to vary spatially, but was kept constant over space. Covariates were scaled to unit standard deviation. In these spatial models, year of collection can be considered a nuisance variable for our present purposes. These models included all specimens with phenotype data.

$$Phenotype_{ij} = \beta_1 year_j + \beta_{2j} AI_j + \beta_{3j} JanMinimum_j + \beta_{4j} AprilMean_j + \mu + error_{ij}$$

In this model, the subscript j denotes location. The errors are assumed to be independent, normally distributed, and have constant variance.

Models were fit in R (version 3.5.0, R Core Team 2011) using the 'gam' function in package mgcv (version 1.8-17, Wood 2011). We allowed the model fitting to penalize covariates to 0 so that covariates weakly associated with phenotypes could be completely removed from the model; thus, using the mgcv package we can achieve model selection through joint penalization of multiple model terms. Coefficients in spatially varying coefficient models represent the individual relationship between each term and phenotype at each geographic point, which we visualized by plotting the estimated coefficients on a map. Each cell in the 100x100 grid model rasters corresponded to 106 km East/West at the lowest latitude (28.16°) and 44km North/South, calculated using Vincenty ellipsoid distances in the geosphere package. Model predictions farther than 200km from a sampled accession were discarded when visualizing results.

We considered two other spatially-varying environmental variables of interest: elevation and N deposition. However, the N deposition estimates we tested (Dentener 2006) were spatially coarse and correlated with year (r^2 = .209). Elevation was not obviously correlated with year (r^2 = .004), but the smooth term for elevation had an estimated concurvity greater than .9 in both the temporal and spatial models, which indicates that it could be approximated from the smooth terms of our other variables. We left elevation and nitrogen deposition covariates out of the final models because inclusion resulted in instability in the numerical routines the GAM software (mgcv) used to estimate parameters and

approximate Hessian matrices needed for confidence intervals. When elevation and nitrogen deposition were included in the model as covariates, the Hessian matrices were not positive definite, and thus could not be used to obtain confidence intervals. We include results in the supplement with elevation but not year for both temporal and spatial models (Figures S13 and S14). Including only variables the three climate covariates and year resulted in numerically stable estimates. In addition, scaling of year and climate variables tended to reduce the concurvity of variables and increase stability.

Finally, we considered how traits covary by fitting GAMs with spatially varying intercepts and measured phenotypes as both response and predictor variables to observe how the correspondence of traits changes through space.

Code for all the models and plots will be included as a supplement and will be available on github.

Results

Distribution of samples through time and space

Samples were broadly distributed, with dense collections in Norway/Sweden, the Netherlands, and Spain (reflecting major herbaria used in the study), and sparser collections in the East.

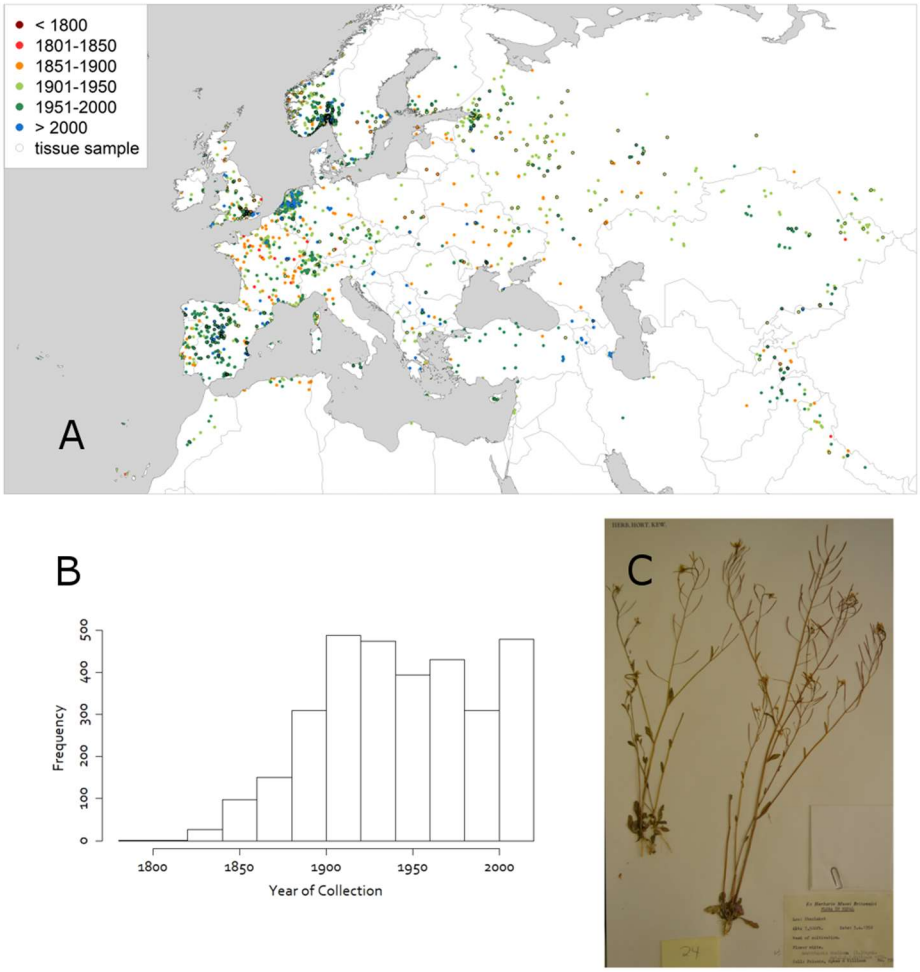

Figure 1: A) Locations of collections used in our analysis. Color of circle corresponds to year of collection. B) Distribution of years of collection. C) Sample herbarium record from Nepal, 1952, with a $\Delta^{13}C$ of 21.9, a $\delta^{15}N$ of 3.6, and a C:N ratio of 23.4.

Correlations among phenotypes

We found generally weak correlations among phenotypes of Arabidopsis individuals. The first two principal components explained only 36.3% and 24.1%, respectively, of the variance in the phenotypes of $\Delta^{13}C$, $\delta^{15}N$, date of collection, C:N, and PTU (N = 397). The first principal component corresponded to a negative correlation between C:N and day of collection (bivariate r = -0.194). Inspecting the relationship between collection date and C:N further, it had a triangle shape (Figure 2B), i.e. there were no late-collected individuals with high C:N. ANOVA showed the slopes of the regression of the 25th and 75th percentiles to be significantly different (p = .00153). The second PC corresponded to a negative correlation between $\Delta^{13}C$ and $\delta^{15}N$ (bivariate r = -.218). C:N and leaf N are highly correlated (bivariate r = -0.815), so we focus on C:N in the text. Leaf N results can be found in the supplement.

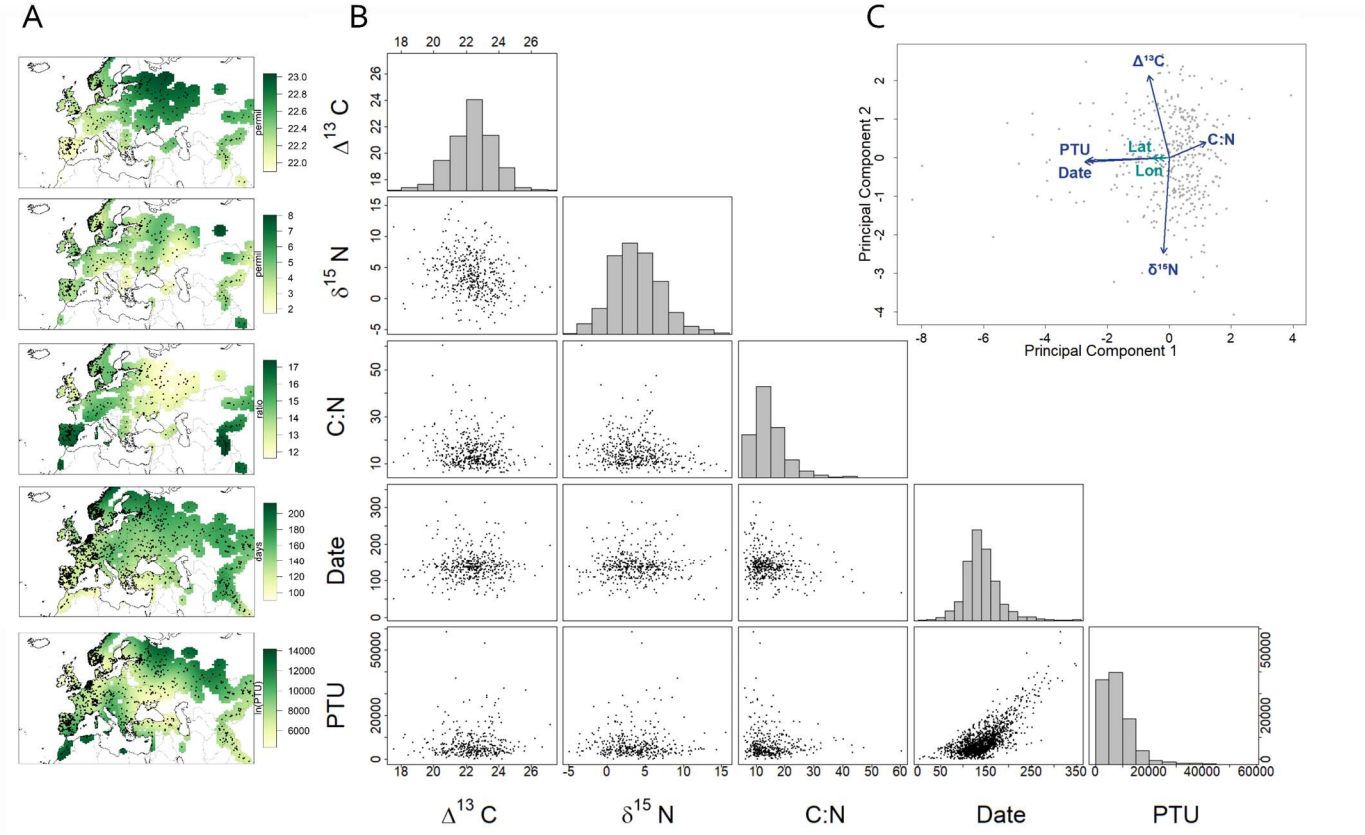

Figure 2: (A) Variation in phenotypes across the native range of Arabidopsis for $\Delta^{13}C$, $\delta^{15}N$, C:N, collection date, and photothermal units (PTU) at collection. Color indicates the fitted mean value of the phenotype. Collection date is earlier in the southwest and Turkey in comparison to other regions; however, PTUs are higher in the southwest and in the northeast. $\delta^{15}N$ is variable across the range. C:N shows a gradient of increasing to the southeast and southwest. $\Delta^{13}C$ increases along a northeasterly gradient. (B) Correlations between phenotypes in this study. There is a positive trend between PTU and date of collection. PCA of phenotypes showed an inverse relationship between C:N and PTU and an inverse relationship between $\Delta^{13}C$ and $\delta^{15}N$ along the first and second principal components (C). Arrows represent correlation of phenotypes with principal components.

Spatial variation in long-term average phenotypes

We visualized spatial diversity in phenotypes by plotting the intercept surfaces in the year only models (Figure 2A). All phenotypes showed significant spatial variation (all GAM smooth terms significant). $\Delta^{13}C$ was lower in the Iberian Peninsula and higher in Russia (GAM smooth term, p = .0002). $\delta^{15}N$ varied across the range, but with less pronounced spatial gradients (GAM smooth term, p = .003). C:N was higher in the Iberian Peninsula and the East and lower in Russia (GAM smooth term, p = 8.24e-05). Collection day was earlier along the Atlantic coast and Mediterranean (GAM smooth term, p = <2e-16). Despite this, PTU at collection still was higher in the Mediterranean region as well as at far northern, continental sites (GAM smooth term, p = <2e-16).

Temporal change in phenotypes

Several phenotypes have changed significantly over the study period (1794-2010, Figure 3 above). For example, C:N ratio increased in later years in much of Southwestern Europe. $\delta^{15}N$ decreased significantly throughout most of the range. Collection date and PTUs became significantly later in many regions from the Mediterranean to Central Asia, although collection date became significantly earlier in the extreme south (Morocco and Himalayas). There was no significant temporal trend in $\Delta^{13}C$ (not shown).

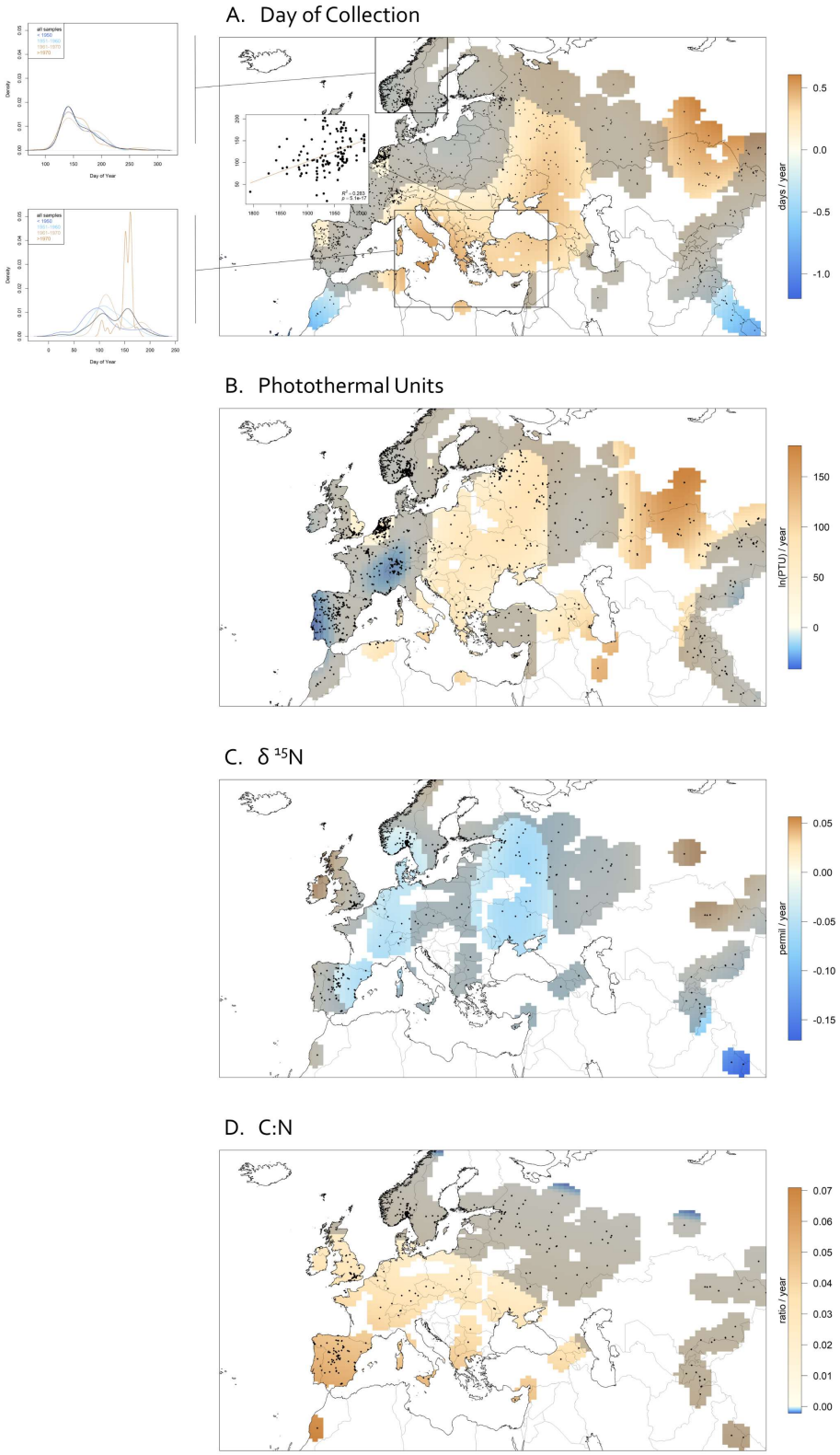

Figure 3, previous page: Change in phenotypes due to year for collection date (A), photothermal units (B), delta nitrogen (C), and C:N (D). Color indicates the value of the coefficient for year in the model excluding climate variables. Day of collection and photothermal units have increased over time in most of the range, but with some exceptions for day of collection in the south. Change in collection day was uneven across regions, with greater shifts in the Aegean than in the Scandinavian Peninsula. $\delta^{15}N$ decreased across most of the range, and C:N increased, most notably in the southwest. Gray shading indicates regions where estimated coefficient is not significantly different from 0. Inset scatterplot in A shows the significant increase in collection date with year for samples in the boxed Mediterranean region. Plots to the left of A show the density of collection dates through the year remains stable through time for Scandinavian collections within the boxed region (top) but shift toward more collections late in the year in the boxed Mediterranean collections (bottom).

Temporal change in phenotypes after accounting for climate anomalies

The temporal trends in phenotypes across the study period were likely partly related to underlying climate variation. However, many of the phenotypes were still significantly associated with year of collection even when accounting for temporal anomalies in climate from 1901-2010. There was a general delay in collection through time in much of the eastern range (Figure S1, S2). However, Iberian collections were significantly earlier in later years. Across most of Europe, later years of collection also were associated with significantly greater C:N ratio (Figures S9, S10). Similarly, we observed $\delta^{15}N$ decreasing in later years across much of Arabidopsis' range, as expected with elevated CO_2 and increased nitrogen deposition. There was still no significant temporal trend in $\Delta^{13}C$.

Phenotype associations with spatiotemporal climate gradients

Date of collection – In years (temporal models) with a relatively warm January or April plants were collected significantly earlier (Figure 4A). Similarly, in locations (spatial models) with warmer temperatures plants were collected earlier, though in many regions these coefficients were non-significant and some exhibited reversed signs. We also tested associations with July aridity index (precipitation/PET) and found that plants were collected significantly earlier in years (temporal models) with dry summers in central/eastern Europe, suggesting a drought escape strategy, but later following dry summers in Central Asia, suggesting a drought avoidance strategy (Figure 4B).

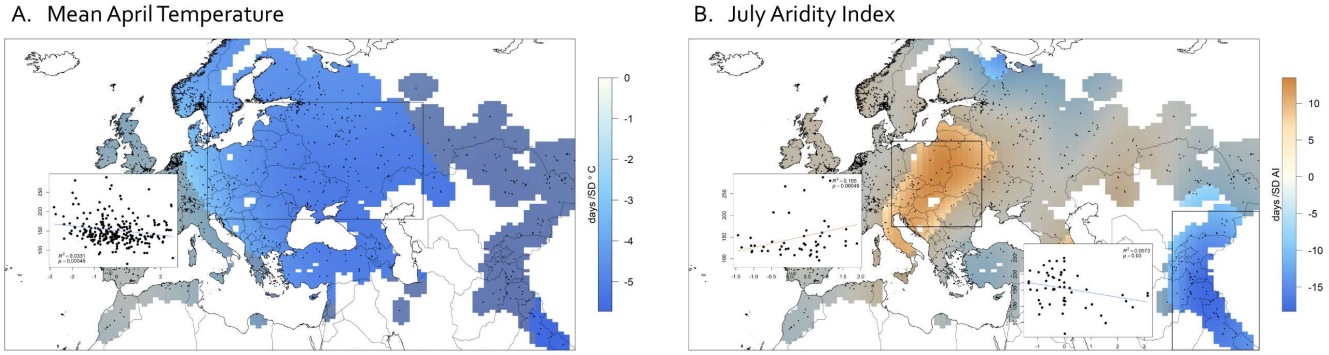

Figure 4: Association between collection day of Arabidopsis thaliana *temporal mean April temperatures (A) and July Aridity Index (B) anomalies (compared to 50-year average). Color indicates the value of the coefficient of the April mean temperature or July Aridity Index term. In years where April was warmer, plants were collected earlier. In wetter years, plants were collected later in Eastern Europe but earlier in Asia. Shading indicates regions where estimated coefficient is not significantly different from 0. Scatterplots of phenotype measures for individuals within the boxed areas show a decreasing collection date with mean April temperature and increasing collection date with July aridity index in Eastern Europe and decreasing collection date in Central Asia.*

Leaf C:N – Leaf C:N was significantly different among locations (spatial models) differing in April mean temperature and January minimum temperature, although the direction of these trends differed among regions. In this model, warmer winters were associated with higher C:N in southwestern Europe but lower C:N in central Asia (Figure S10B) and warmer temperatures in April predicted lower C:N in Iberia. For the temporal model, plants collected in wetter years in Iberia had significantly higher C:N ratios.

Photothermal units – To standardize spatiotemporal variation in developmental periods, we also modeled climate associations with PTUs. As expected if PTUs account for most of the environmental control on development, there were few areas where temperature anomalies were significantly associated with PTUs (Figure S3). However, in some areas, accumulated PTUs at collection changed significantly in association with spatial temperature gradients, suggesting greater complexity in phenology beyond PTU models (Figure S4). Locations with warmer Aprils were collected at more PTUs around the Baltic sea and fewer PTUs around the Aegean. In the temporal model, accessions from Western Europe, Greece, and Central Asia, had lower PTUs in wetter years and accessions in Central Europe had higher PTUs wetter years. In the spatial model, accessions from wetter areas in the south had lower PTUs, but this pattern was reversed in the North (Figure S3, S4).

Δ ^{13}Carbon – Although we expected moisture limitation would lead to stomatal closure and lower $\Delta^{13}C$,, the coefficient for summer aridity was not significantly different from 0 anywhere in either the temporal or spatial models of $\Delta^{13}C$. However, there was regional significance in the spatial relationship between $\Delta^{13}C$ and long-term mean April temperature (smooth term significance: p = 1.58e-5). Specifically, in Central Asia areas with warmer Aprils had higher $\Delta^{13}C$ than collections from areas with cooler Aprils (Figure S6A). In Iberia and Northeastern Europe, the reverse was true (though the local relationships were not significant).

Including elevation caused estimation of confidence intervals to be unreliable, so elevation was left out of the final models, but elevation tended to have a negative relationship with $\Delta^{13}C$ as expected due to declining C_a at high elevation (Körner *et al.* 1988) (Figures S13 and S14). This was significant in the temporal model across much of Asia.

***δ* ^{15}Nitrogen** – $\delta^{15}N$ was positively significantly related to temporal anomalies in July Aridity Index in a number of regions (Figure S7), but this relationship was heterogenous across space. The relationship was positive in Iberia, Asia, and Central Europe, but negative in the North of France. Temperature was only significantly related to $\delta^{15}N$ in the case of spatial variation in minimum January temperatures around the North Sea.

Covariance of phenotypes

In a GAM where C:N was a function of date or accumulated photothermal units, we found both measures of phenology were negatively correlated with C:N across the Arabidopsis native range, but this was insignificant at the 95% confidence interval when the effect of year was included (Figure S20). $\Delta^{13}C$ was likewise insignificantly correlated with date of collection and accumulated photothermal units when accounting for year (Figure S20).

Discussion

Widely distributed species often exhibit considerable phenotypic diversity, a large portion of which may be driven by adaptive plastic and evolutionary responses to environmental gradients. The existence of genetic variation in environmental responses among populations suggests that responses to temporal environmental shifts may differ dramatically among populations. Previous studies of intraspecific trait variation in response to environment have tended to focus on genetic variation of environmental responses in common gardens (*e.g.* Wilczek *et al.* 2009; Kenney *et al.* 2014), temporal trends in phenology from well-monitored sites (CaraDonna *et al.* 2014), or field sampling of individuals from a small number of sites (Jung *et al.* 2010) Here, we build upon this work to study change in traits across an entire species range over two centuries, giving us a window into drivers of intraspecific diversity and regional differences in global change biology. From the accumulated work of field biologists contained in natural history collections, we found later flowering times and higher accumulated photothermal units over the study period across most of the range and lower δ ^{15}nitrogen and higher C:N in more recent collections. Additionally, we observed distinct regional differences in phenology, Δ ^{13}carbon, and C:N in response to rainfall and temperature. However, we observed insignificant covariance among phenotypes in space.

Phenology

We found strong gradients in two measures of phenology suggesting adaptive responses to climate drive intraspecific phenotypic diversity. Years and locations that were warmer than average in either April or January corresponded to significantly earlier collection dates, consistent with temperature's positive effect on growth rate (Wilczek *et al.* 2009). The fact that these relationships were spatially variable, and insignificant in some regions, may indicate areas of contrasting phenological response, perhaps due to lost vernalization signal or variable effects on germination (Burghardt *et al.* 2016). Alternatively, Arabidopsis is known to complete a generation within a growing season, climate permitting, and warmer climates allow for fall flowering (Wilczek *et al.* 2009; Fournier-Level *et al.* 2013). If warmer temperatures enable a greater number of spring or summer germinants to flower before winter in regions such as Central Europe, we would expect to see later collection dates in more recent years (Burghardt *et al.* 2015). In this case, regions that have earlier collection dates with warmer temperature may be limited in generational cycles due to another environmental factor, such as summer drought or short growing seasons. Our models provided support that some phenological variation did reflect seasonality of moisture availability. We found Arabidopsis was collected significantly earlier in years with dry summers in central Europe and at significantly lower PTU in regions of wet summers around the Mediterranean, suggesting drought escape or avoidance strategies could be important in those regions. Alternatively, later collections in wetter years could be the result of multiple successful generations due to the extra rainfall.

Our findings of later collection dates through the study period (1798-2010) may surprise some readers due to previously observed acceleration of temperate spring phenology (Parmesan & Yohe 2003). However, we modeled changes in mean phenological response to environment, which can be weakly related to phenology of extreme individuals (e.g. first-flowering individuals) (CaraDonna *et al.* 2014). Why might Arabidopsis flower later even as global temperatures rise? First, non-climate environmental changes (*e.g*. in land use) may drive phenology. Second, changes in climate or atmospheric pCO_2 may favor alternate life histories. As described above, later collections in more recent years might represent an increasing proportion of fast-growing spring or summer annuals as opposed to winter annuals.

Physiology, leaf economics spectrum

We found little evidence for tight coordination among studied phenotypes, fitting with some past surveys that found weak to no support for a single major axis in intraspecific trait variation in response to environment (e.g. Albert *et al.* 2010; Wright & Sutton-Grier 2012). Common garden experiments often find substantial genetic covariation between these traits possibly due to pleiotropy or selection maintaining correlated variation (Kenney *et al.* 2014). The massively complex environmental variation organisms experience in the wild may combine with genotype-by-environment interactions to generate high dimensional variation among individuals in nature.

Nevertheless, we found that plants collected later in the year have low leaf C:N, indicative of a fast-growing resource acquisitive strategy. This strategy may be adaptive for rapid-cycling plants germinating and flowering within a season (spring/summer annuals), contrasted with slower-growing genotypes known to require vernalization for flowering over a winter annual habit. Indeed, Des Marais et al. (2013) found that vernalization requiring (likely winter annual) Arabidopsis genotypes had lower leaf N than genotypes not requiring vernalization for flowering, the latter of which could also behave as spring or summer annuals.

However, the Leaf Economic Spectrum and fast/slow life history frameworks do not well explain our C:N models in response to climate variables, which were insignificant across regions for both spatial and temporal climate gradients of temperature and aridity. This may be due to the intraspecific nature of our study, as opposed to the interspecific basis for LES. In multispecies analyses, phenotype correlations with climate may be influenced by community composition changes across the environment or may not represent the physiology or climate niche of a given species (Albert *et al.* 2010; Elmore *et al.* 2017). However, as additional environmental processes drive leaf nitrogen in the wild, our study may have lacked power to differentiate the effects of nitrogen acquisition and efficiency traits from the effects of geochemistry. This may be especially true for $\delta^{15}N$, which neither decreased with rainfall nor responded to temperature as expected, but did decrease with year as previously reported in multi-species surveys (Craine *et al.* 2009; McLauchlan *et al.* 2010).

Similarly, we did not see strong relationships between aridity and $\Delta^{13}C$. $\Delta^{13}C$ was expected to be closely related to environmental conditions of rainfall and temperature due to stomatal gas exchange dynamics (Farquhar *et al.* 1989; Diefendorf *et al.* 2010). While surprising, $\Delta^{13}C$ patterns may be weaker than expected for a couple of reasons. First, we observed both positive and negative trends for aridity and date of collection, consistent with the hypothesis that Arabidopsis exhibits both drought escaping and drought avoiding genotypes. The phenological responses to moisture might limit $\Delta^{13}C$ responses by allowing consistent favorable conditions during growth periods. Second, gas exchange and carbon assimilation depend in part on leaf architecture and physiology traits like venation, specific leaf area (SLA), and leaf N (Schulze *et al.* 2006; Brodribb *et al.* 2007; Easlon *et al.* 2014), which could mitigate the $\Delta^{13}C$ response we observe. For instance, as SLA increases in areas of high rainfall (expected according to LES (Reich *et al.* 2003)), the photosynthetic rate could be impacted. In addition, genetic variation in these traits may affect $\delta^{13}C$, and thus in turn $\Delta^{13}C$, differently in spring and winter annuals (Easlon *et al.* 2014). Furthermore, water use efficiency, for which $\Delta^{13}C$ serves as an indicator, is not limited to leaf traits but could also reflect root investment or other traits unmeasured here. The lack of $\Delta^{13}C$ patterns could also be the effect of elevated atmospheric CO_2 (Drake *et al.* 2017), although limiting the model to observations before 1950 (when atmospheric CO_2 was much lower) suggested, surprisingly, that Asian accessions growing in locations of high Aridity Index may have had decreased $\Delta^{13}C$. Investigating at a

smaller scale the patterns we found could clarify mechanisms leading to the phenotype-climate associations or lack thereof. Smaller scales would benefit in addressing populations known to be genetically unique, as in Iberian relicts (Alonso-Blanco *et al.* 2016), that may cause unexpected regional differences in phenotype trends (Figure S1D).

Our approach, technical problems to surmount in future studies

Understanding how spatiotemporal environmental variation drives the intraspecific diversity that exists in broadly distributed species has been challenging due to the scale of the problem. However, advances in digitization of museum specimens and the generation of global gridded spatiotemporal environmental data are opening a new window into large scale patterns of biodiversity. One challenge of herbarium specimens is that they are typically mature (reproductive) individuals. Thus, these specimens contain limited information on phenology and physiology at earlier life stages, which can have subsequently strong impacts on later observed stages. Use of developmental models (Burghardt *et al.* 2015) might allow one to backcast potential developmental trajectories using herbarium specimens and climate data, to make predictions about phenology of germination and transition to flowering.

Generalized additive models are a flexible approach to model phenotype responses to environment that might differ spatially among populations (MacGillivray *et al.* 2010). Herbarium records represent imperfect and biased samples of natural populations, and future efforts may benefit from additional information that might allow us to account for these biases. Here, we sampled a very large number of specimens across continents and decades and so we deem it unlikely that most of the patterns we observed were driven by biases associated with specific collectors. Nevertheless, as museum informatics advance it may become possible to explicitly model potential sources of bias, for example those arising from collecting behavior of specific researchers.

Conclusion

Widely distributed species often harbor extensive intraspecific trait diversity. Natural history collections offer a window into this diversity and in particular allow investigation of long-term responses to anthropogenic change across species ranges. Here we show that spatiotemporal climate gradients explain much of this diversity but nevertheless much of the phenotypic diversity in nature remains to be explained.

Acknowledgements

Hundreds of botanists collected the specimens studied here. The staff at herbaria at Oslo Natural History Museum, Kew Gardens, Real Jardin Botanico, Komarov Botanical Garden, and the British Museum of Natural History gave permission for tissue sampling. Michelle Brown provided essential assistance in collecting herbarium tissue. Jason Bonette helped coordinate sample preparation. Major assistance in digitizing of specimens was provided by Patrick Herné. Eugene Shakirov aided in translating Russian specimen labels. Data from the MNHN in Paris were obtained thanks to the participatory science program Les Herbonautes" (MNHN/Tela Botanica) which is part of Infrastructure Nationale e-RECOLNAT: ANR-11-INBS-0004. Additional volunteers from the Atlas of Living Australia helped with digitization and georeferencing. Funding was provided by an Earth Institute fellowship to JRL.

References

Albert, C.H., Thuiller, W., Yoccoz, N.G., Soudant, A., Boucher, F., Saccone, P., *et al.* (2010). Intraspecific functional variability: extent, structure and sources of variation. *J. Ecol.*, 98, 604–613.

Alonso-Blanco, C., Andrade, J., Becker, C., Bemm, F., Bergelson, J., Borgwardt, K.M.M., *et al.* (2016). 1,135 genomes reveal the global pattern of polymorphism in Arabidopsis thaliana. *Cell*, 166, 481–491.

Amundson, R., Austin, A.T., Schuur, E.A.G., Yoo, K., Matzek, V., Kendall, C., *et al.* (2003). Global patterns of the isotopic composition of soil and plant nitrogen. *Global Biogeochem. Cycles*, 17.

Blonder, B., Violle, C., Bentley, L.P. & Enquist, B.J. (2011). Venation networks and the origin of the leaf economics spectrum. *Ecol. Lett.*, 14, 91–100.

Both, C., Artemyev, A. V., Blaauw, B., Cowie, R.J., Dekhuijzen, A.J., Eeva, T., *et al.* (2004). Large-scale geographical variation confirms that climate change causes birds to lay earlier. *Proc. R. Soc. B Biol. Sci.*, 271, 1657–1662.

Brachi, B., Faure, N., Horton, M., Flahauw, E., Vazquez, A., Nordborg, M., *et al.* (2010). Linkage and association mapping of *Arabidopsis thaliana* flowering time in nature. *PLoS Genet.*, 6, 40.

Brodribb, T.J., Feild, T.S. & Jordan, G.J. (2007). Leaf maximum photosynthetic rate and venation are linked by hydraulics. *Plant Physiol.*, 144, 1890–1898.

Burghardt, L.T., Edwards, B.R. & Donohue, K. (2016). Multiple paths to similar germination behavior in *Arabidopsis thaliana*. *New Phytol.*, 209, 1301–1312.

Burghardt, L.T., Metcalf, C.J.E., Wilczek, A.M., Schmitt, J. & Donohue, K. (2015). Modeling the influence of genetic and environmental variation on the expression of plant life cycles across landscapes. *Am. Nat.*, 185, 212–227.

CaraDonna, P.J., Iler, A.M. & Inouye, D.W. (2014). Shifts in flowering phenology reshape a subalpine plant community. *Proc. Natl. Acad. Sci.*, 111, 4916–4921.

Chardon, F., Barthélémy, J., Daniel-Vedele, F. & Masclaux-Daubresse, C. (2010). Natural variation of nitrate uptake and nitrogen use efficiency in *Arabidopsis thaliana* cultivated with limiting and ample nitrogen supply. *J. Exp. Bot.*, 61, 2293–2302.

Craine, J.M., Elmore, A.J., Aidar, M.P.M., Bustamante, M., Dawson, T.E., Hobbie, E.A., *et al.* (2009). Global patterns of foliar nitrogen isotopes and their relationships with climate, mycorrhizal fungi, foliar nutrient concentrations, and nitrogen availability. *New Phytol.*, 183, 980–992.

Davis, C.C., Willis, C.G., Connolly, B., Kelly, C. & Ellison, A.M. (2015). Herbarium records are reliable sources of phenological change driven by climate and provide novel insights into species' phenological cueing mechanisms. *Am. J. Bot.*, 102, 1599–1609.

Dentener, F.J. (2006). Global maps of atmospheric nitrogen deposition, 1860, 1993, and 2050. *ORNL DAAC*.

Diefendorf, A.F., Mueller, K.E., Wing, S.L., Koch, P.L. & Freeman, K.H. (2010). Global patterns in leaf ^{13}C discrimination and implications for studies of past and future climate. *Proc. Natl. Acad. Sci.*, 107, 5738–5743.

Drake, B.L., Hanson, D.T., Lowrey, T.K. & Sharp, Z.D. (2017). The carbon fertilization effect over a century

of anthropogenic CO_2 emissions: higher intracellular CO_2 and more drought resistance among invasive and native grass species contrasts with increased water use efficiency for woody plant. *Glob. Chang. Biol.*, 23, 782–792.

Easlon, H.M., Nemali, K.S., Richards, J.H., Hanson, D.T., Juenger, T.E. & McKay, J.K. (2014). The physiological basis for genetic variation in water use efficiency and carbon isotope composition in *Arabidopsis thaliana*. *Photosynth. Res.*, 119, 119–129.

Elmore, A.J., Craine, J.M., Nelson, D.M. & Guinn, S.M. (2017). Continental scale variability of foliar nitrogen and carbon isotopes in *Populus balsamifera* and their relationships with climate. *Sci. Rep.*, 7.

Evans, J.R. (1989). Photosynthesis and nitrogen relationships in leaves of C3 plants. *Oecologia*, 78, 9–19.

Farquhar, G., O'Leary, M. & Berry, J. (1982). On the relationship between carbon isotope discrimination and the intercellular carbon dioxide concentration in leaves. *Aust. J. Plant Physiol.*, 9, 121–137.

Farquhar, G.D., Ehleringer, J.R. & Hubick, K.T. (1989). Carbon isotope discrimination and photosynthesis. *Annu. Rev. Plant Physiol. Plant Mol. Biol.*, 40, 503–537.

Fournier-Level, A., Wilczek, A.M., Cooper, M.D., Roe, J.L., Anderson, J., Eaton, D., *et al.* (2013). Paths to selection on life history loci in different natural environments across the native range of *Arabidopsis thaliana*. *Mol. Ecol.*, 22, 3552–3566.

Hijmans, R.J. (2017). geosphere: spherical trigonometry.

Hijmans, R.J., Cameron, S.E., Parra, J.L., Jones, P.G. & Jarvis, A. (2005). Very high resolution interpolated climate surfaces for global land areas. *Int. J. Climatol.*, 25, 1965–1978.

Hoffmann, M.H. (2002). Biogeography of *Arabidopsis thaliana* (L.) Heynh. (Brassicaceae). *J. Biogeogr.*, 29, 125–134.

Jung, V., Violle, C., Mondy, C., Hoffmann, L. & Muller, S. (2010). Intraspecific variability and trait-based community assembly. *J. Ecol.*, 98, 1134–1140.

Kenney, A.M., Mckay, J.K., Richards, J.H. & Juenger, T.E. (2014). Direct and indirect selection on flowering time, water-use efficiency (WUE, $\delta^{13}C$), and WUE plasticity to drought in *Arabidopsis thaliana*. *Ecol. Evol.*, 4, 4505–4521.

Körner, C., Farquhar, G.D. & Roksandic, Z. (1988). A global survey of carbon isotope discrimination in plants from high altitude. *Oecologia*, 74, 623–632.

Lang, P.L.M., Willems, F.M., Scheepens, J.F., Burbano, H.A. & Bossdorf, O. (2018). Using herbaria to study global environmental change. *PeerJ Prepr.*

Lasky, J.R., Forester, B.R. & Reimherr, M. (2018). Coherent synthesis of genomic associations with phenotypes and home environments. *Mol. Ecol. Resour.*, 18, 91–106.

Lasky, J.R., Des Marais, D.L., McKay, J.K., Richards, J.H., Juenger, T.E. & Keitt, T.H. (2012). Characterizing genomic variation of *Arabidopsis thaliana*: the roles of geography and climate. *Mol. Ecol.*, 21, 5512–5529.

Ludlow, M.M. (1989). Strategies of response to water stress. In: *Structural and functional responses to environmental stresses: water shortage* (eds. Kreeb, K.H., Richter, H. & Hinckley, T.M.). SPB Academic Publishers, Berlin, pp. 269–281.

MacGillivray, F., Hudson, I.L. & Lowe, A.J. (2010). Herbarium collections and photographic images: Alternative data sources for phenological research. In: *Phenological Research: Methods for Environmental and Climate Change Analysis*. Springer Netherlands, Dordrecht, pp. 425–461.

Des Marais, D.L., Hernandez, K.M. & Juenger, T.E. (2013). Genotype-by-environment interaction and plasticity: exploring genomic responses of plants to the abiotic environment. *Annu. Rev. Ecol. Evol. Syst.*, 44, 5–29.

McCarroll, D. & Loader, N.J. (2004). Stable isotopes in tree rings. *Quat. Sci. Rev.*, 23, 771–801.

McLauchlan, K.K., Ferguson, C.J., Wilson, I.E., Ocheltree, T.W. & Craine, J.M. (2010). Thirteen decades of foliar isotopes indicate declining nitrogen availability in central North American grasslands. *New Phytol.*, 187, 1135–1145.

Miller-Rushing, A.J., Primack, R.B., Primack, D. & Mukunda, S. (2006). Photographs and herbarium specimens as tools to document phenological changes in response to global warming. *Am. J. Bot.*, 93, 1667–1674.

New, M., Hulme, M. & Jones, P. (2000). Representing twentieth-century space-time climate variability. Part II: Development of 1901-96 monthly grids of terrestrial surface climate. *J. Clim.*, 13, 2217–2238.

Nienhuis, J., Sills, G.R., Martin, B. & King, G. (1994). Variance for water-use efficiency among ecotypes and recombinant inbred lines of *Arabidopsis thaliana* (Brassicaceae). *Am. J. Bot.*, 81, 943–947.

Ordoñez, J.C., Van Bodegom, P.M., Witte, J.P.M., Wright, I.J., Reich, P.B. & Aerts, R. (2009). A global study of relationships between leaf traits, climate and soil measures of nutrient fertility. *Glob. Ecol. Biogeogr.*, 18, 137–149.

Pardo, L.H., McNulty, S.G., Boggs, J.L. & Duke, S. (2007). Regional patterns in foliar ^{15}N across a gradient of nitrogen deposition in the northeastern US. *Environ. Pollut.*, 149, 293–302.

Parmesan, C. & Yohe, G. (2003). A globally coherent fingerprint of climate change impacts across natural systems. *Nature*, 421, 37–42.

R Core Team. (2018). R: a language and environment for statistical computing.

Rachmilevitch, S., Cousins, A.B. & Bloom, A.J. (2004). Nitrate assimilation in plant shoots depends on photorespiration. *Proc. Natl. Acad. Sci.*, 101, 11506–11510.

Reich, P.B. (2014). The world-wide "fast-slow" plant economics spectrum: a traits manifesto. *J. Ecol.*, 102, 275–301.

Reich, P.B., Hungate, B.A. & Luo, Y. (2006). Carbon-nitrogen interactions in terrestrial ecosystems in response to rising atmospheric carbon dioxide. *Annu. Rev. Ecol. Evol. Syst.*, 37, 611–636.

Reich, P.B. & Oleksyn, J. (2004). Global patterns of plant leaf N and P in relation to temperature and latitude. *Proc. Natl. Acad. Sci.*, 101, 11001–11006.

Reich, P.B., Wright, I.J., Cavender-Bares, J., Craine, J.M., Oleksyn, J., Westoby, M., *et al.* (2003). The evolution of plant functional variation: traits, spectra, and strategies. *Int. J. Plant Sci.*, 164, S143–S164.

Sack, L., Scoffoni, C., McKown, A.D., Frole, K., Rawls, M., Havran, J.C., *et al.* (2012). Developmentally based scaling of leaf venation architecture explains global ecological patterns. *Nat. Commun.*, 3,

837.

Schulze, E.D., Turner, N.C., Nicolle, D. & Schumacher, J. (2006). Leaf and wood carbon isotope ratios, specific leaf areas and wood growth of *Eucalyptus* species across a rainfall gradient in Australia. *Tree Physiol.*, 26, 479–492.

Stock, W.D. & Evans, J.R. (2006). Effects of water availability, nitrogen supply and atmospheric CO_2 concentrations on plant nitrogen natural abundance values. *Funct. Plant Biol.*, 33, 219–227.

Stocking, C.R. & Ongun, A. (1962). The intracellular distribution of some metallic elements in leaves. *Am. J. Bot.*, 49, 284–289.

United Nations Environment Program. (1997). *World atlas of desertification*. 2nd edn.

Wheeler, D.C. & Waller, L.A. (2009). Comparing spatially varying coefficient models: a case study examining violent crime rates and their relationships to alcohol outlets and illegal drug arrests. *J. Geogr. Syst.*, 11, 1–22.

Wilczek, A.M., Cooper, M.D., Korves, T.M. & Schmitt, J. (2014). Lagging adaptation to warming climate in *Arabidopsis thaliana*. *Proc. Natl. Acad. Sci.*, 111, 7906–7913.

Wilczek, A.M., Roe, J.L., Knapp, M.C., Cooper, M.D., Lopez-Gallego, C., Martin, L.J., *et al.* (2009). Effects of genetic perturbation on seasonal life history plasticity. *Science (80-.).*, 323, 930–934.

Willis, C.G., Ellwood, E.R., Primack, R.B., Davis, C.C., Pearson, K.D., Gallinat, A.S., *et al.* (2017). Old plants, new tricks: phenological research using herbarium specimens. *Trends Ecol. Evol.*, 32, 531–546.

Wood, S.N. (2006). *Generalized additive models: an introduction with R*. *Texts Stat. Sci.* 1st edn. Chapman and Hall/CRC.

Wood, S.N. (2011). Fast stable restricted maximum likelihood and marginal likelihood estimation of semiparametric generalized linear models. *J. R. Stat. Soc. Ser. B Stat. Methodol.*, 73, 3–36.

Wright, I.J., Reich, P.B., Westoby, M., Ackerly, D.D., Baruch, Z., Bongers, F., *et al.* (2004). The worldwide leaf economics spectrum. *Nature*, 428, 821–827.

Wright, J.P. & Sutton-Grier, A. (2012). Does the leaf economic spectrum hold within local species pools across varying environmental conditions? *Funct. Ecol.*, 26, 1390–1398.

Zhu, Y., Siegwolf, R.T.W., Durka, W. & Körner, C. (2010). Phylogenetically balanced evidence for structural and carbon isotope responses in plants along elevational gradients. *Oecologia*, 162, 853–863.

Additional plots of model surfaces
Phenology

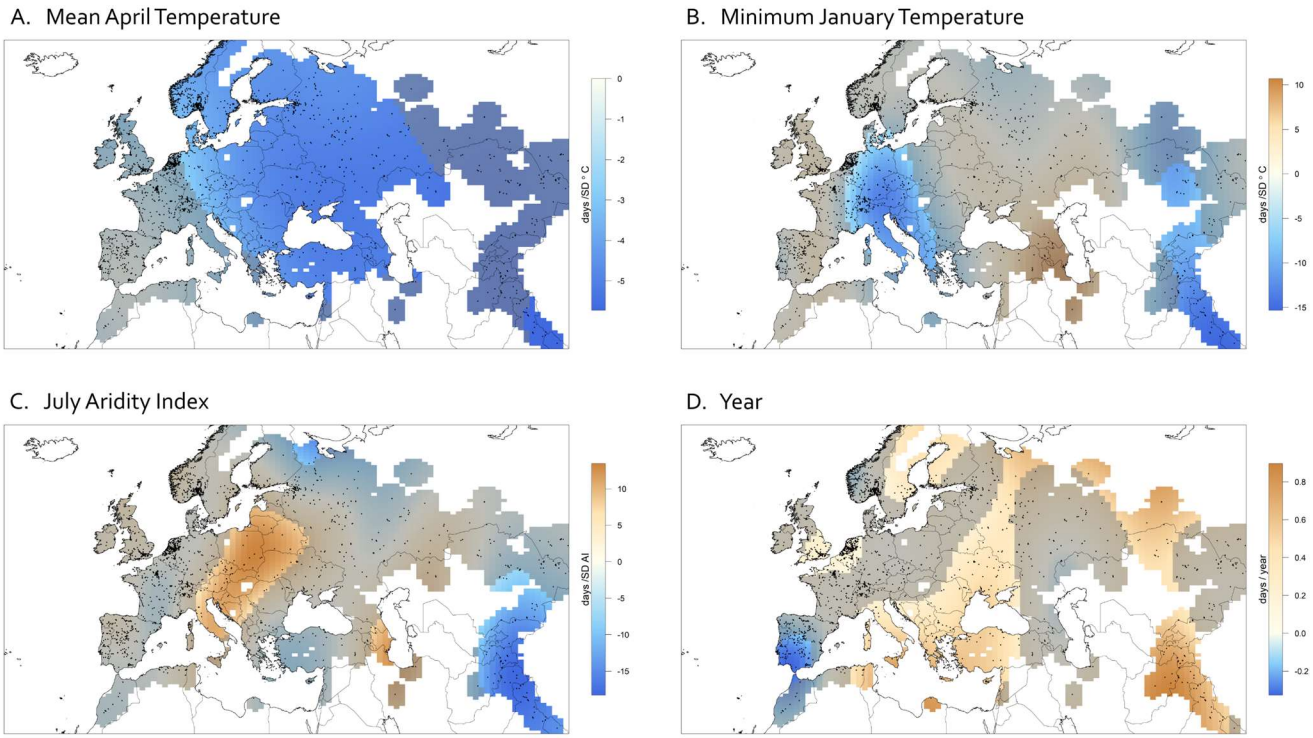

Figure S1: Temporal model phenology for April mean temperature (A), January minimum temperature (B), July aridity index (C), and year (D).

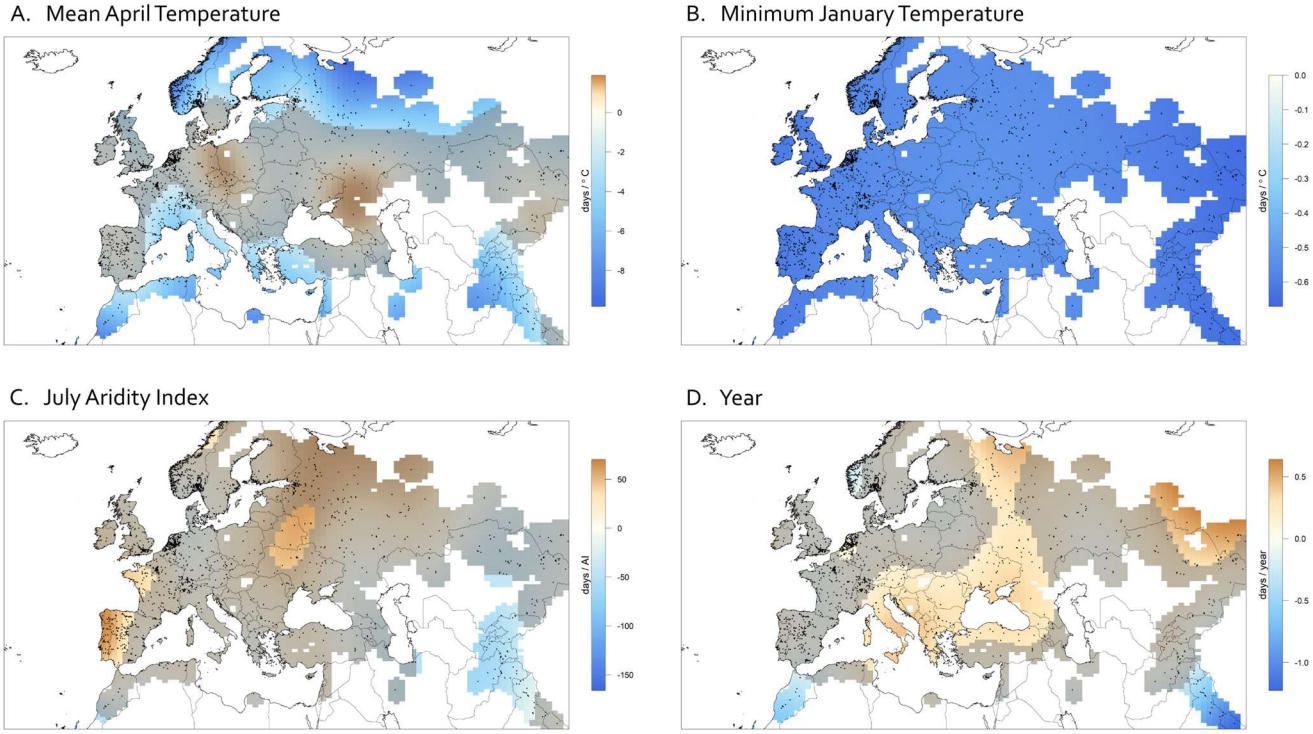

Figure S2: Spatial model phenology for April mean temperature (A), January minimum temperature (B), July aridity index (C), and year (D).

Photothermal Units

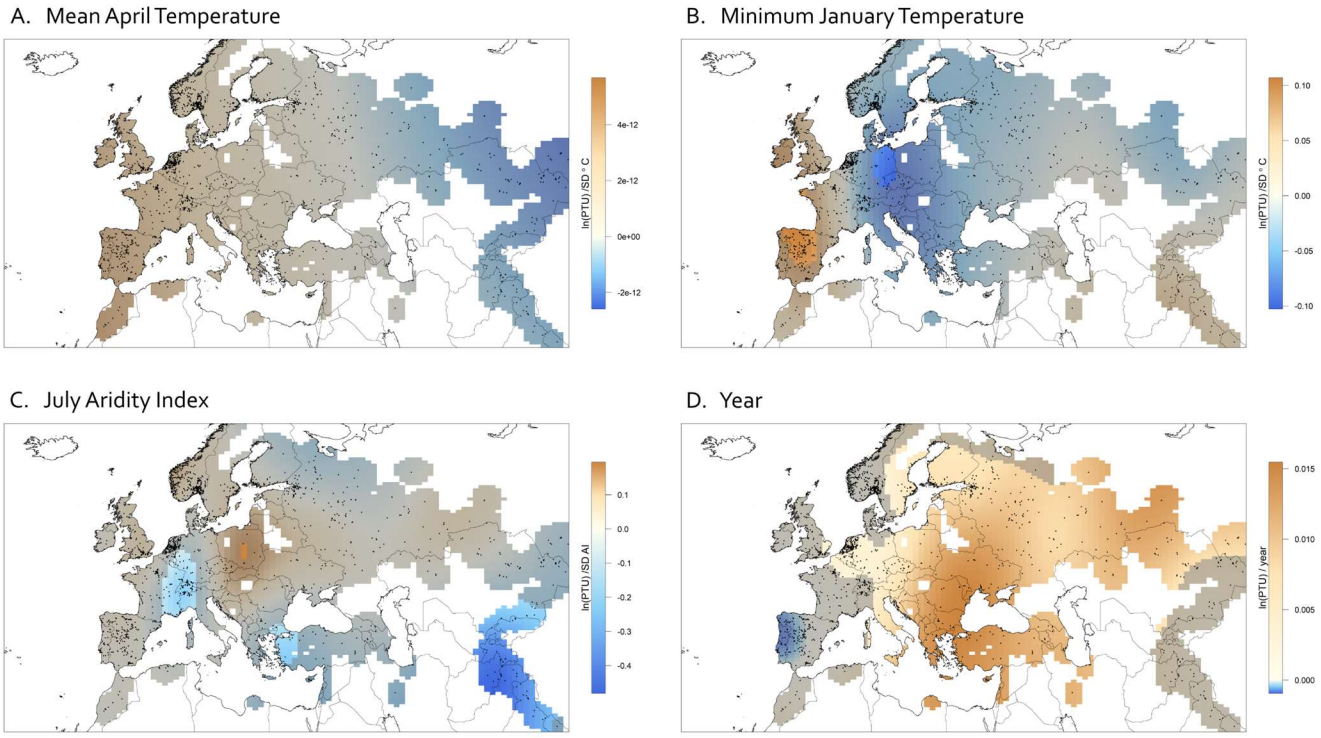

Figure S3: Temporal model photothermal units for April mean temperature (A), January minimum temperature (B), July aridity index (C), and year (D).

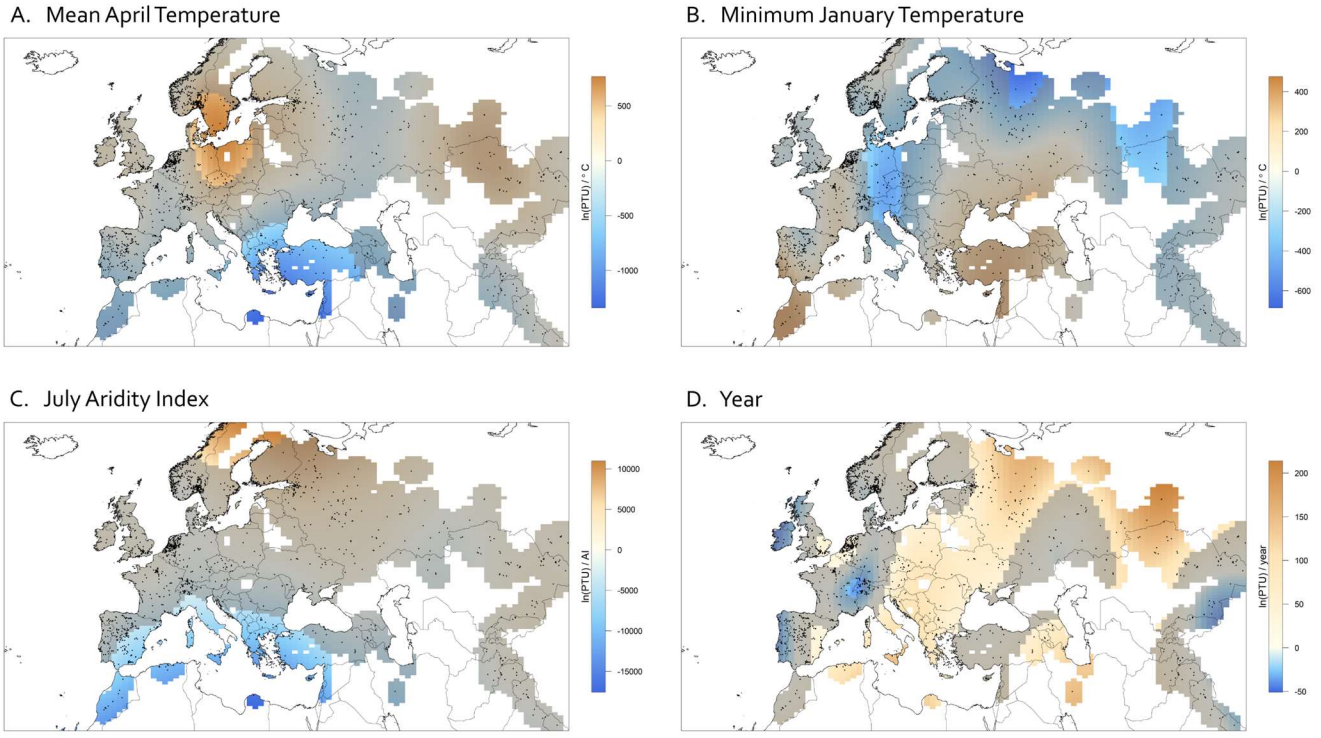

Figure S4: Spatial model photothermal units for April mean temperature (A), January minimum temperature (B), July aridity index (C), and year (D).

$\Delta^{13}C$

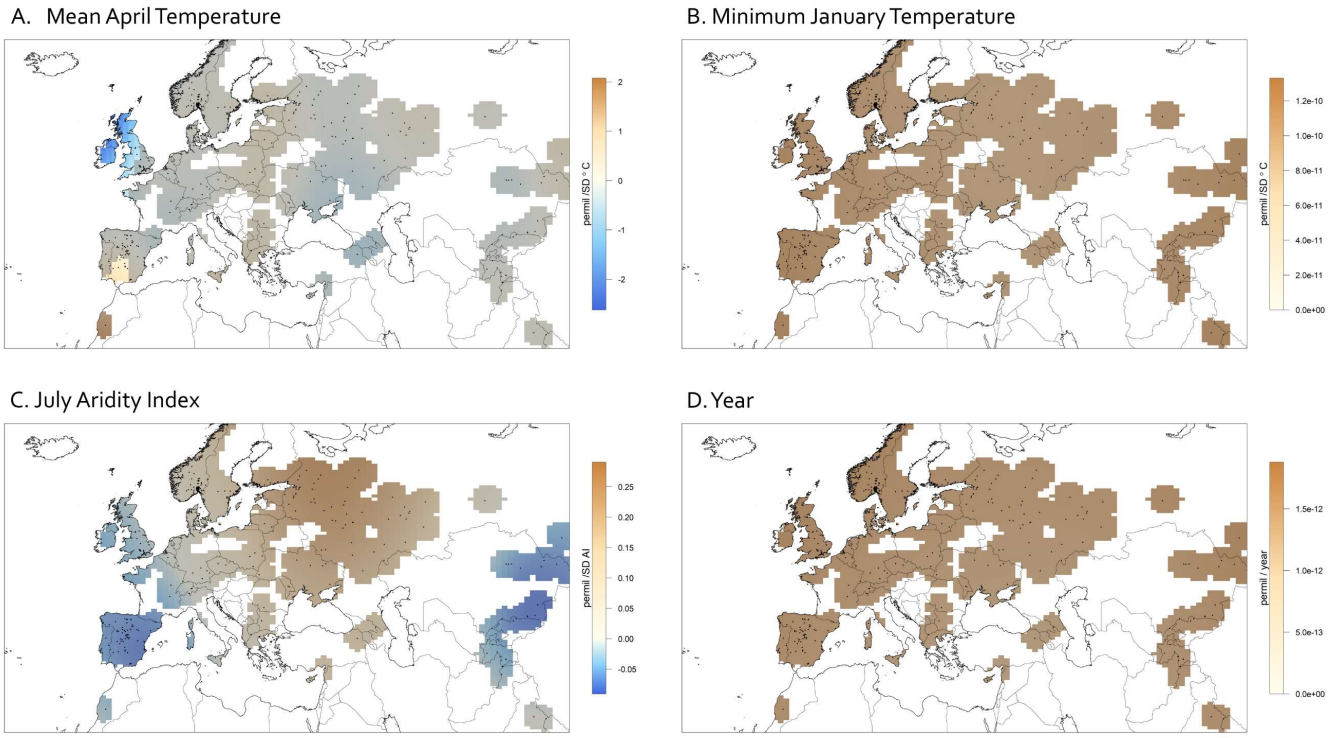

Figure S5: Temporal model $\Delta^{13}C$ for April mean temperature (A), January minimum temperature (B), July aridity index (C), and year (D).

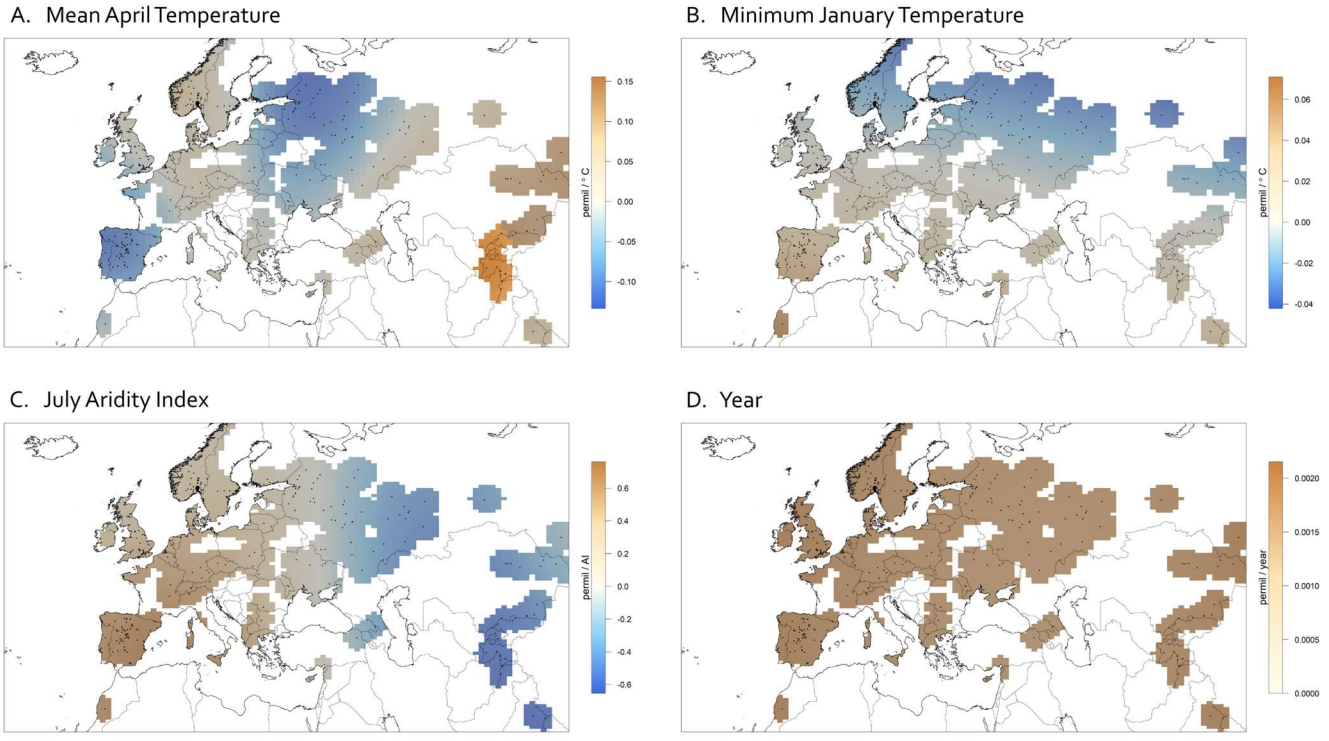

Figure S6: Spatial model $\Delta^{13}C$ for April mean temperature (A), January minimum temperature (B), July aridity index (C), and year (D).

$\delta^{15}N$

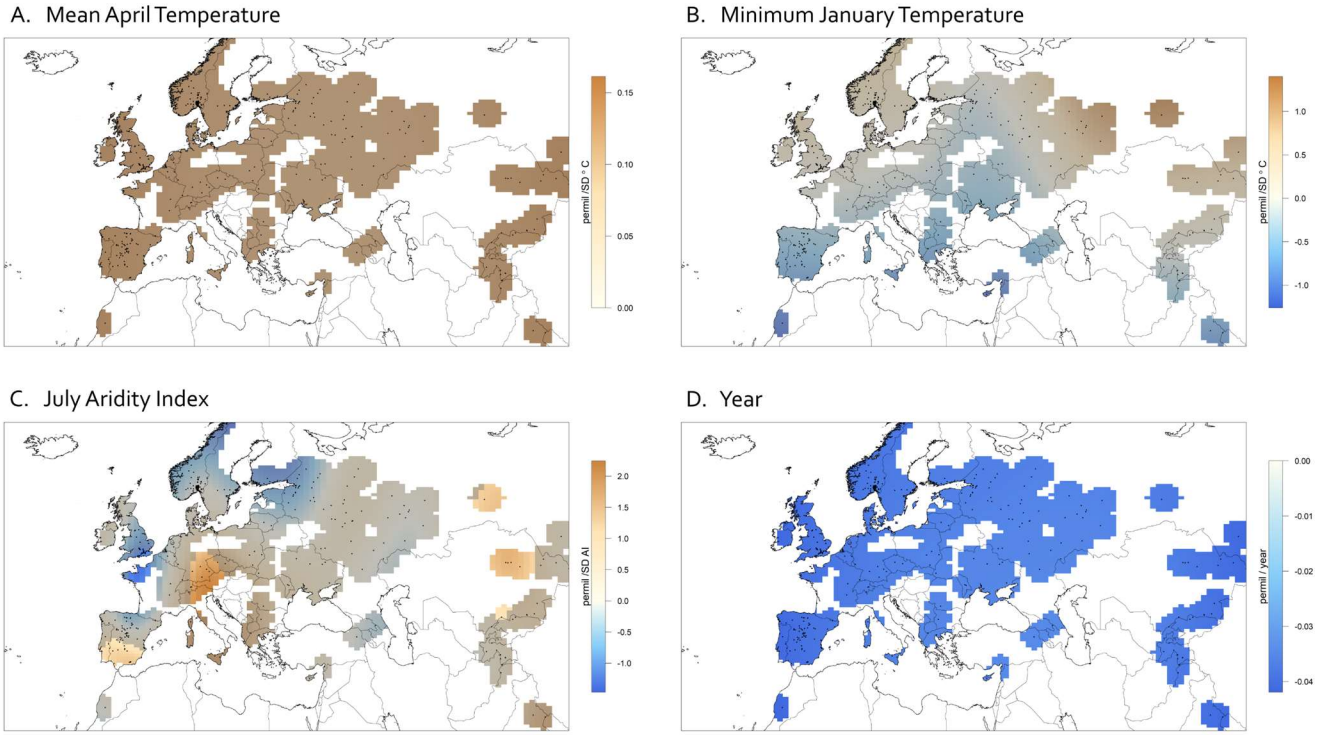

Figure S7: Temporal model for $\delta^{15}N$ April mean temperature (A), January minimum temperature (B), July aridity index (C), and year (D).

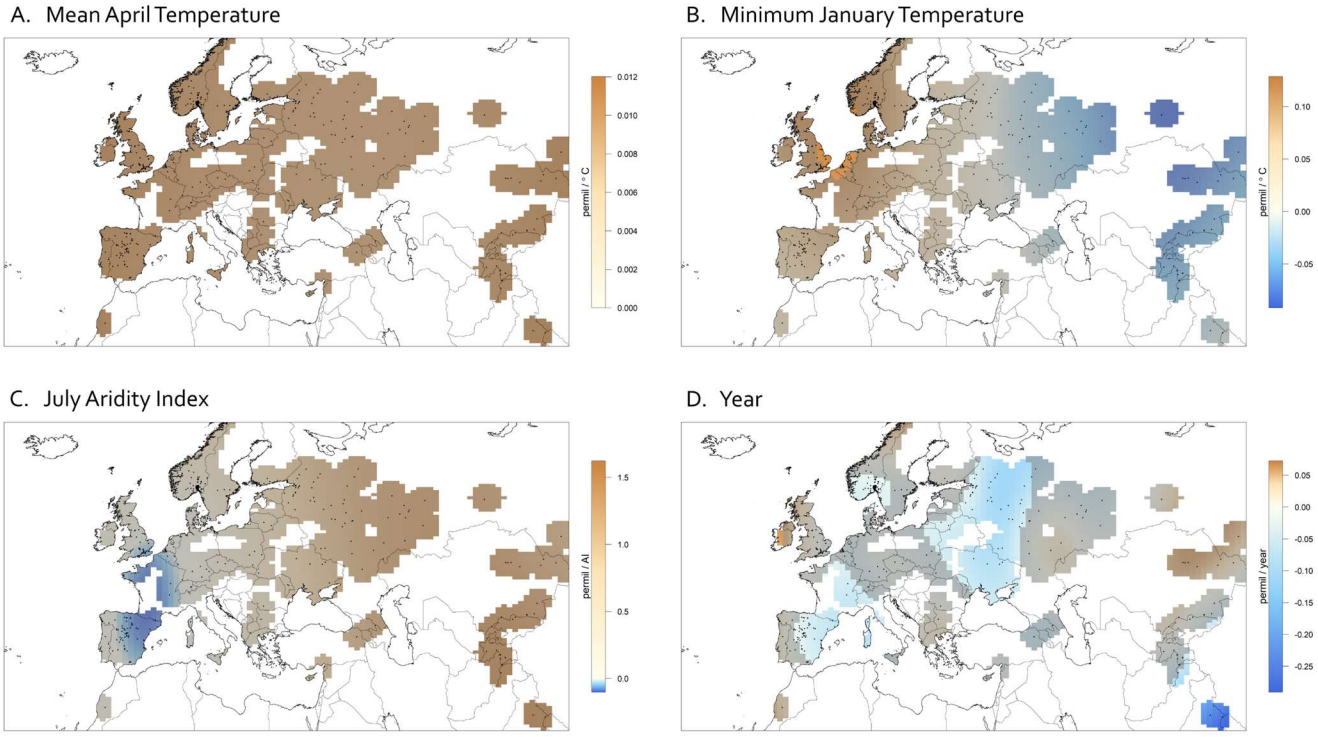

Figure S8: Spatial model $\delta^{15}N$ for April mean temperature (A), January minimum temperature (B), July aridity index (C), and year (D).

C:N

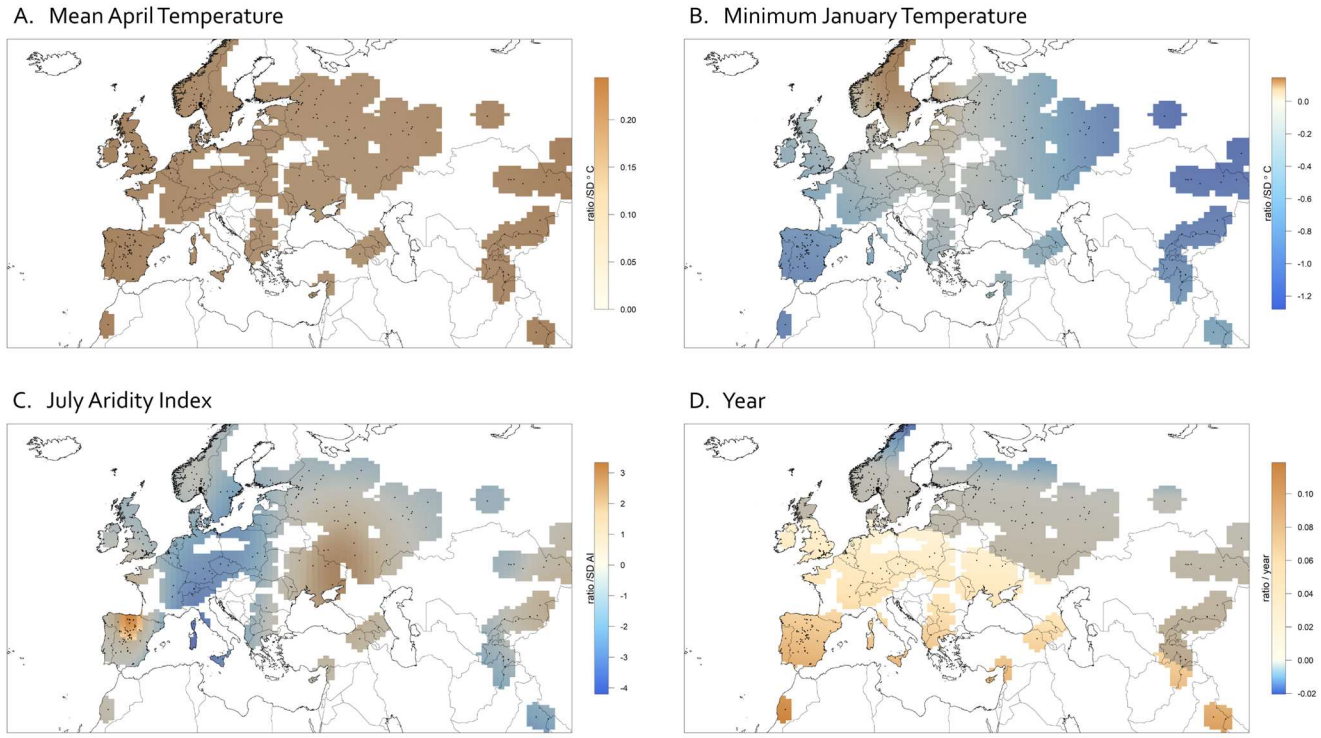

Figure S9: Temporal model for C:N April mean temperature (A), January minimum temperature (B), July aridity index (C), and year (D).

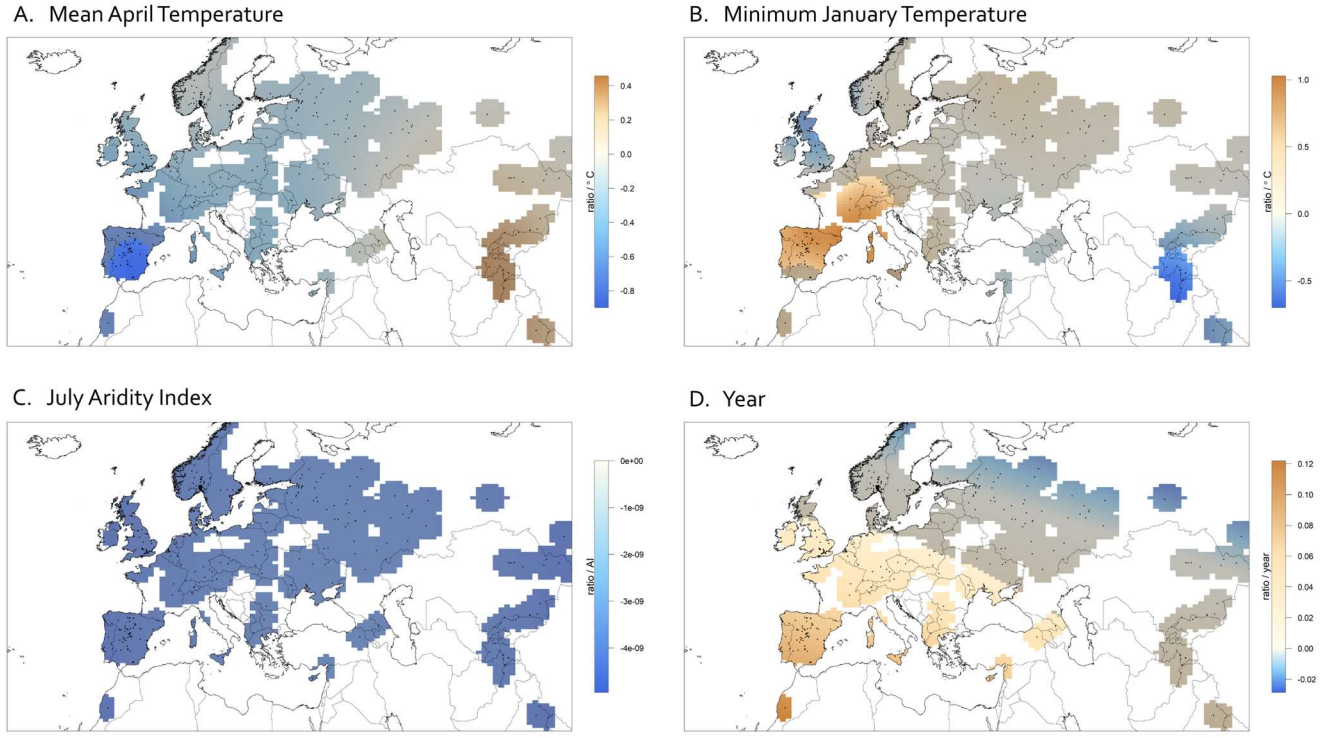

Figure S10: Spatial model C:N for April mean temperature (A), January minimum temperature (B), July aridity index (C), and year (D).

Proportion N. Note: the Hessian Matrix was not positive definite for these matrices, so the confidence intervals are unreliable.

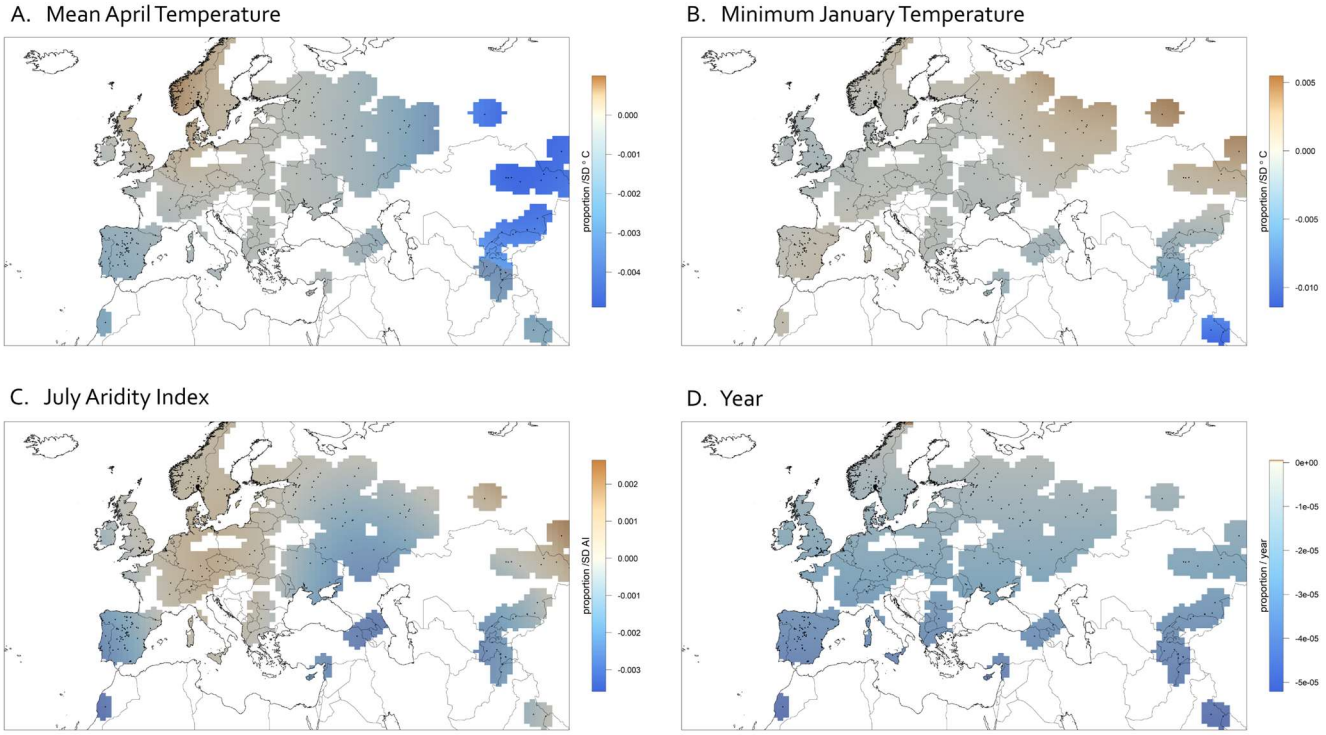

Figure S11: Anomaly model proportion N for April mean temperature (A), January minimum temperature (B), July aridity index (C), and year (D).

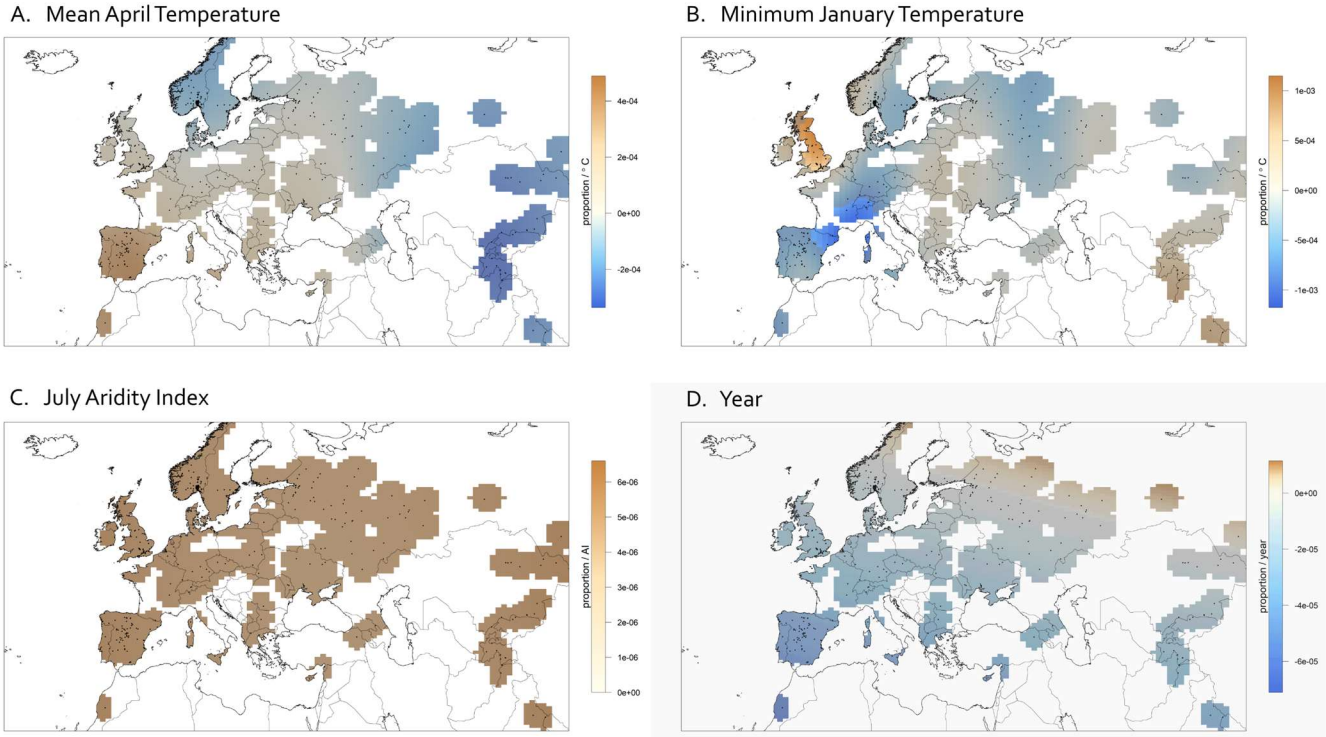

Figure S12: Spatial model proportion N for April mean temperature (A), January minimum temperature (B), July aridity index (C), and year (D).

$\Delta^{13}C$ using elevation in place of year

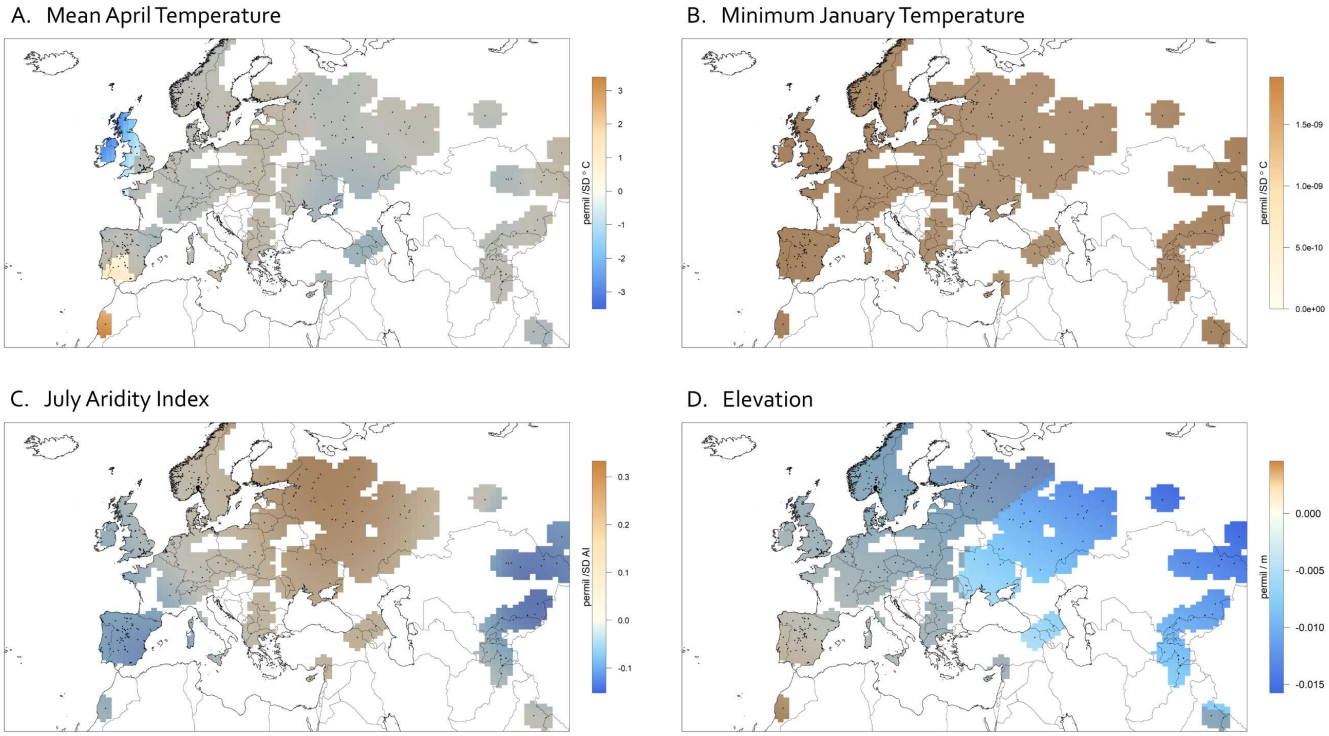

Figure S13: Anomaly model $\Delta^{13}C$ for April mean temperature (A), January minimum temperature (B), July aridity index (C), and elevation (D).

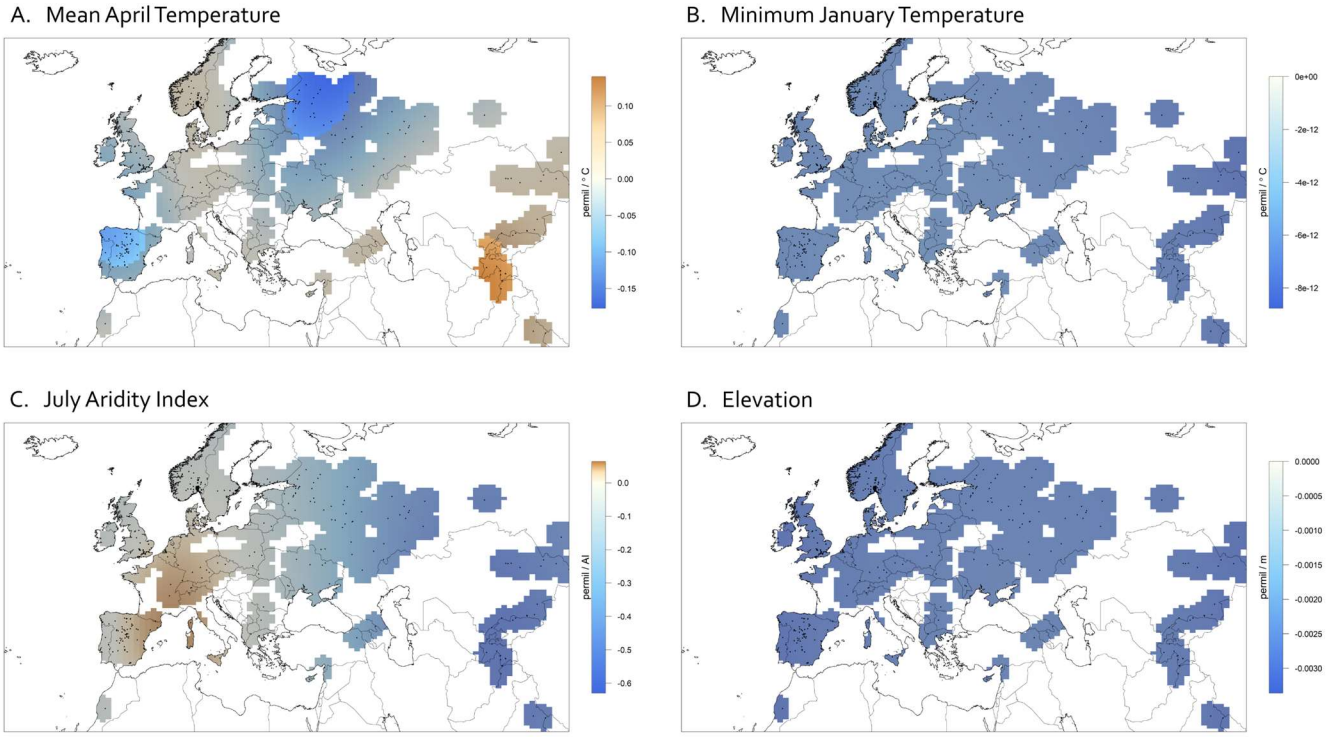

Figure S14: Spatial model $\Delta^{13}C$ for April mean temperature (A), January minimum temperature (B), July aridity index (C), and elevation (D).

$\Delta^{13}C$ using only samples collected before 1950. Rising atmospheric CO_2 concentrations may mask climate associations (Drake *et al.* 2017). However, $\Delta^{13}C$ before 1950 is still not significantly related to climate for the anomaly model or the year only model, and the spatial model indicates a negative association between $\Delta^{13}C$ and Aridity in the eastern part of the native range.

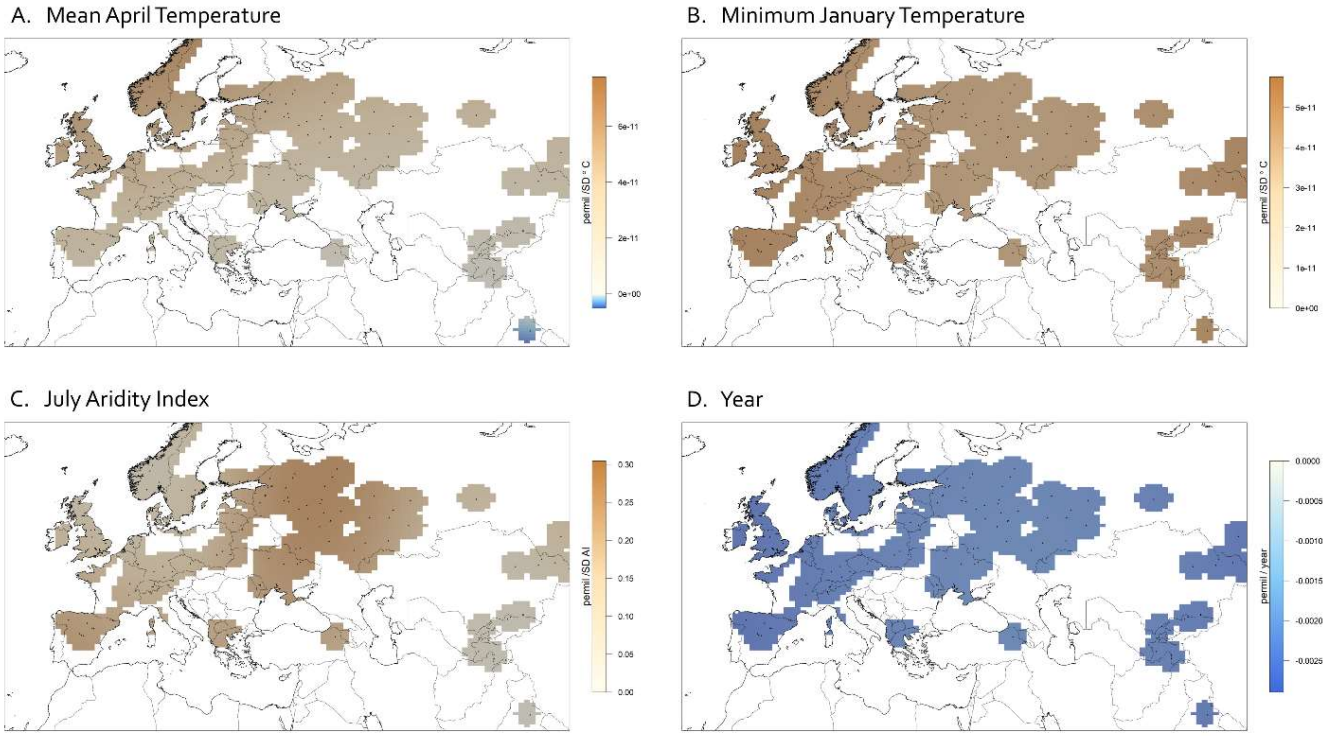

Figure S15: Anomaly model $\Delta^{13}C$ for April mean temperature (A), January minimum temperature (B), July aridity index (C), and year (D) for samples collected prior to 1950.

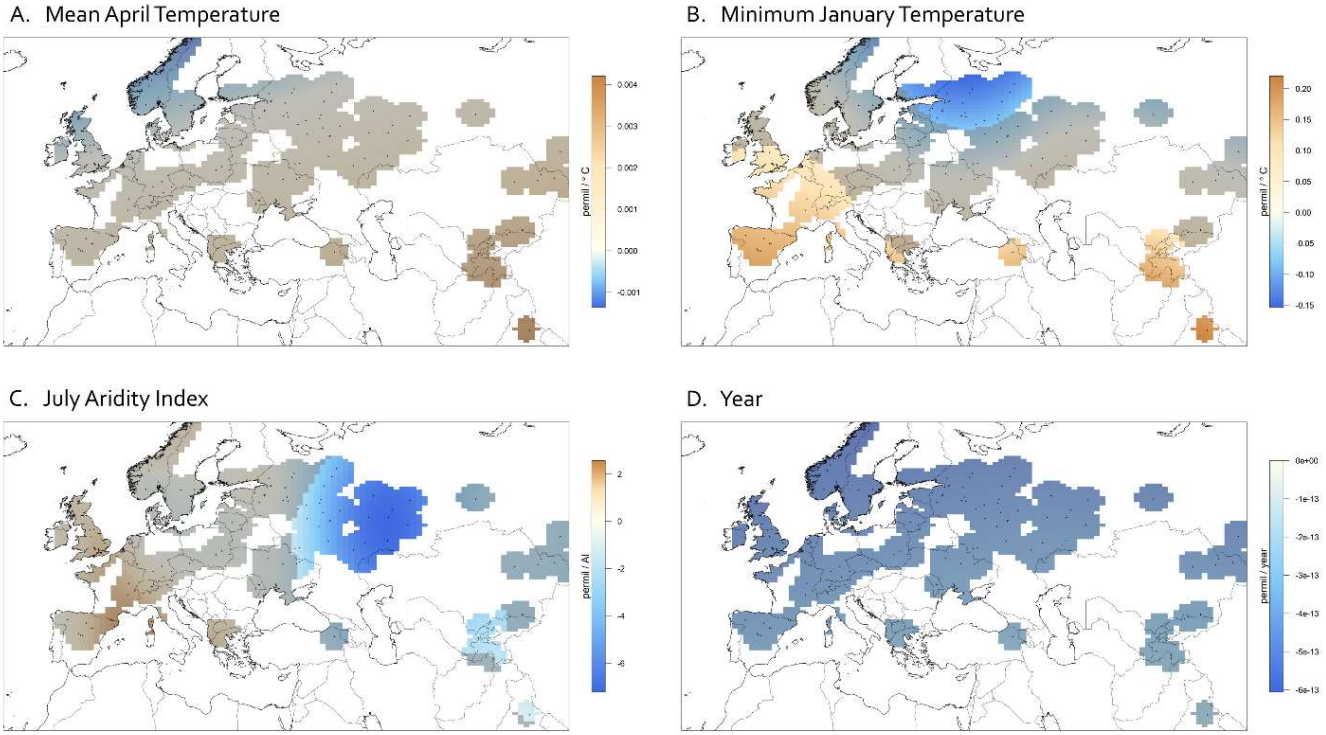

Figure S16: Spatial model $\Delta^{13}C$ for April mean temperature (A), January minimum temperature (B), July aridity index (C), and year (D for samples collected prior to 1950).

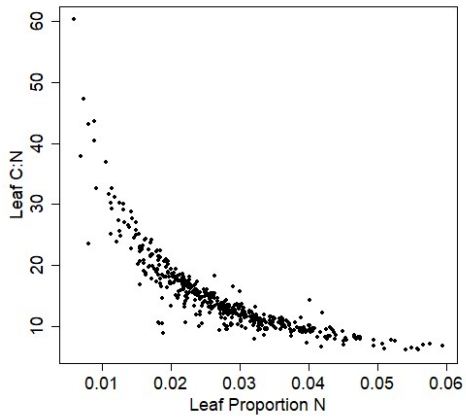

Figure S17: Proportion leaf nitrogen and leaf C:N ratio of the accessions sampled in our study show a negative association.

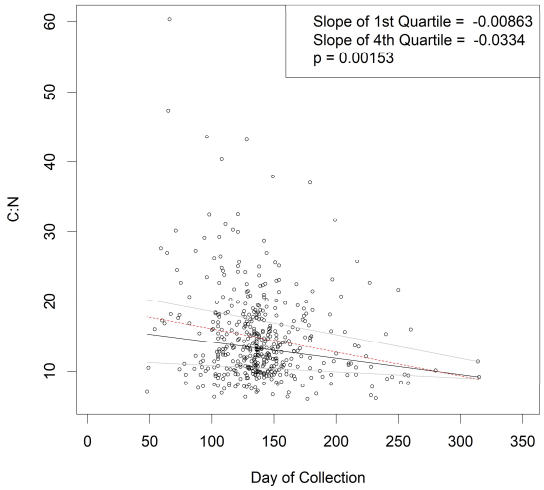

Figure S18: Quantile regression for C:N predicted by day of collection. No late collected accessions have a high C:N ratio.

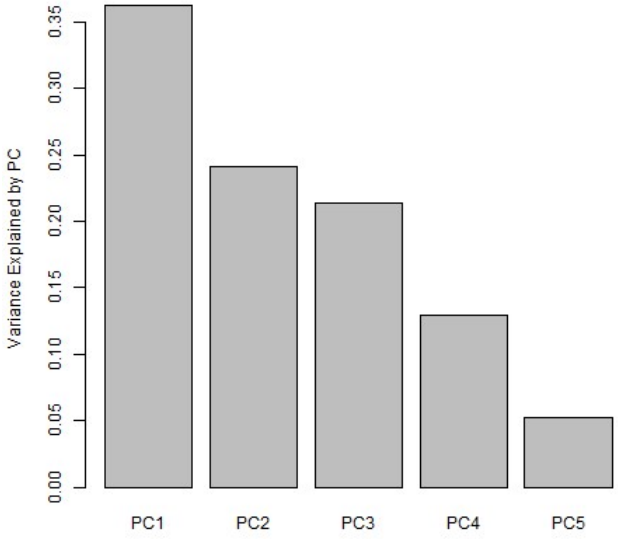

Figure S19: Proportion of variance explained by Principal Components analysis of phenotypes

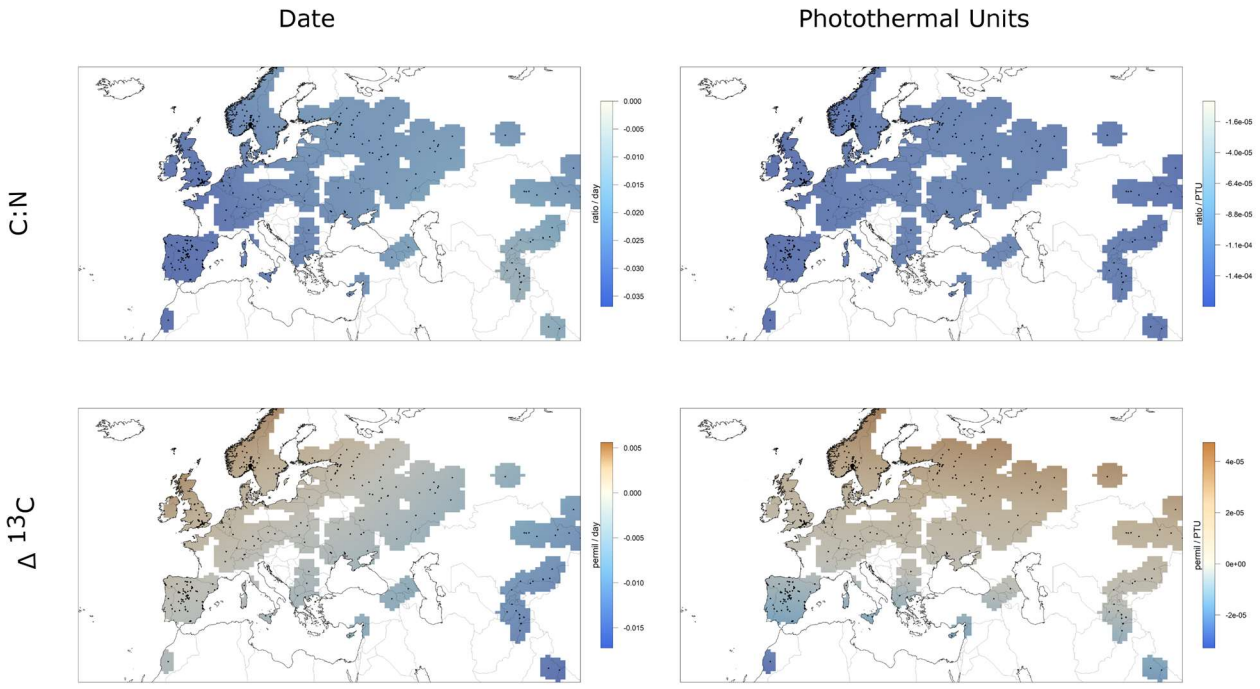

Figure S20: Covariance of phenotypes. Across space, the relationship between C:N and date or PTU at collection is not significantly negative across the range. $\Delta^{13}C$ may be positively related to days or PTU at collection in some regions and negatively related to days or PTU at collection in other regions, but the relationship does not differ significantly from 0 at the 95% confidence interval.

Isotope measurement methods, continued:

Samples were combusted at 1000°C and ^{13}C and ^{15}N were measured with a PDZ Europa ANCA-GSL elemental analyzer interfaced to a PDZ Europa 20-20 isotope ratio mass spectrometer. Samples were run on plates with two laboratory standards similar in composition to our material and calibrated against NIST Standard Reference Materials. Reference gases were included to calculate isotope ratios. $\Delta^{13}C$ and $\delta^{15}N$ were described relative to the Vienna PeeDee Belemnite and Air international standards.

Elevation

Elevation was acquired from SRTM and WorldClim when SRTM records were missing. Yearly nitrogen deposition values were an interpolation of Dentener 2006's nitrogen deposition model. Code for interpolation included with other scripts.